Institute of Geochemistry, Mineralogy and Mineral
Resources, Faculty of Science, Charles University in Prague

# Alkali-silica reaction of aggregates in real concrete and mortar specimens

**PhD Thesis**

**Mgr. Šárka Lukschová**

**Supervisor: Doc. Mgr. Richard Přikryl, Dr.**
**Advisor: Prof. RNDr. Zdeněk Pertold, CSc.**

**2008**

**Acknowledgements**

The contents section of this thesis is in actual fact shorter than would be the list of persons who I would like to acknowledge here. Before acknowledging some by name, I would like to thank everyone who has somehow contributed to this work in some way. I especially want to express my thanks to my supervisor Dr. Doc. Mgr. Richard Přikryl, for many productive hints, and all the help he has offered me during the work on my thesis. Many thanks also to Prof. RNDr. Zdeněk Pertold, CSc., for discussions held many times throughout the last four years. Thanks as well to Ing. Jan Hromádko, Ing. Tomáš Míčka, and Ing. Jan Horský, for their help with concrete diagnostics. With all my heart, I thank my mother, grandmother and grandfather, and especially to the person closest to me, Radek Šachl, for all that which cannot be expressed in words.

This study was undertaken as a part of Project No. 1F45C/096/120, supported by the Ministry of Transport of the Czech Republic. Financing from the Project No. MSM0021620855 "Material flow mechanisms in the upper spheres of the Earth" is also acknowledged.

I hereby declare that I have developed this thesis entirely on my own. If any other previously published results were used, they are included in the list of references. I permit the lending of this thesis to anyone to whom it may be of interest. I confirm that this work (as well as any significant portion) has not been used to obtain any academic degree, elsewhere.

Date:

Signature

## Abstract

Dissolution and leaching of silica in high alkaline conditions can lead to the formation of alkali-silica gels. These are capable of swelling and thus to deteriorate the concrete. The process known as the alkali-silica reaction (ASR) is exhibited by the formation of a crack network, white and/or transparent coatings, and concrete pulverization. Mitigation of ASR is considered in the use of aggregates containing alkali-non-reactive forms of silica. This can be achieved through extensive knowledge about aggregates, their petrographic characteristics and their ASR potential. This PhD thesis aims to connect a petrographic investigation of aggregates with methods determining their ASR potential in real concrete structures, as well as in experimental mortar specimens.

From concrete samples taken from several concrete bridges and one crash barrier, all located in the Czech Republic, the ASR was investigated using petrographic methods, such as optical microscopy, petrographic image analysis, and scanning electron microscopy combined with an energy dispersive spectrometer (SEM/EDS method); all with the objective to determine the extent of ASR and to identify alkali-reactive aggregates.

Similar petrographic methods were applied to natural aggregates (quartz sands and gravels exploited in the areas around the Cidlina, Dyje, Ohře, Sázava and, mainly, Labe river areas), and to mortar specimens composed of the same aggregates, with the objective to quantify the ASR potential of aggregates, to identify the alkali-reactive components, and to investigate the ASR products. The use of the mortar bar method and the gel pat test enabled quantification of the ASR potential of aggregates, as well as preparation of suitable experimental specimens for the investigation of signs of ASR.

Chert-rich limestones (identified in concrete samples taken from a crash barrier) are regarded to be the most reactive rock type among the investigated aggregates. The very fine-grained siliceous (chert) component in limestones is well known for its high ASR potential. The ASR caused by chert-rich limestones is exhibited by ASR cracks, as well as a large number of pore voids, both partially filled by alkali-silica gels. These chert-rich limestones were regarded to be the primary reason for the ASR in this concrete crash barrier. The chert-rich limestones of 4.0 - 7.0 vol. % enhanced the formation of alkali-silica gels to the volume of 2.3 - 4.9 vol. %. Due to the difficulty in the identification of silica in limestone aggregates, one cannot eliminate some additional content of silica from other limestone particles contained in the concrete samples forming 22.0 - 27.4 vol. %.

Quartz-rich aggregates (*e.g.* quartz-rich sediments, meta-sediments and other metamorphic rocks) represent the most widespread group of investigated aggregates. Their medium ASR potential was experimentally determined in mortar specimens, and by using petrographic image analysis on real concrete structures. Their ASR potential was found to be highly dependent on external conditions (*e.g.* accelerating solutions used in the aggregate test methods) and the time factor. The time factor affecting the concrete structures was compared to the degree of ASR (expressed by the volume of alkali-silica gels) in the concrete samples. The most intensive ASR was observed in concrete samples taken from bridge construction from the 1$^{st}$ half of 20$^{th}$ century, showing alkali-silica gels in a volume of 0.5 – 0.9 vol. % and intensive ASR cracks intruding the aggregates.

A very low degree of ASR was observed in connection with magmatic rocks, especially with basaltic rocks, serpentinites and granitoids. These rock types were mainly identified in concrete samples, forming the main component of the coarse aggregates.

Comparison of those alkali-silica gels in concrete samples with those from mortar bar specimens pointed-out several important factors, such as the time factor and external parameters (composition of accelerating solutions in the case of mortar specimens), affecting the ASR. This conclusion, well known in literature, but partially forgotten in practice, is regarded as important in future research focused upon ASR in the Czech Republic.

This study is acutely focused on the assessment of ASR of quartz-rich natural aggregates, which had not previously been studied in the Czech Republic. Along with conventional microscopic investigation, deformational phenomena including recrystallization, deformation, and grain size were related to the ASR potential of the studied sands. Extremely fine-grained quartz fragments, originating at the boundaries of older quartz, are considered to be responsible for ASR. In contrast, well-crystallized coarse-grained quartz fragments show minimal signs of ASR. The origin of fine-grained young generations of quartz could therefore be responsible for increasing the ASR potential of initially low alkali-reactive rocks, such as monomineral quartz fragments and some magmatic and metamorphic rocks. The comparison of recrystallization signs and the ASR potential of quartz aggregates were carried-out quantitatively on aggregates from several mortar bar specimens and qualitatively on concrete samples. For greater statistical rigor, it is to analyze larger numbers of aggregates contained in concrete samples and/or experimentally tested.

This study also contributes to an exploration of possible applications of some advanced petrographic techniques (including petrographic image analysis and study by SEM/EDS) for the detection of ASR products, and an overall petrographic assessment of laboratory specimens used for laboratory dilation tests (mortar bar specimens). A modification of the conventionally used mortar bar method (following the ASTM C1260 standard) by an after-test petrographic investigation of mortar bar specimens was incorporated into the updated version of the Czech Technical Regulation TP 137 (the complex of methods regulating aggregates testing for ASR in the Czech Republic).

# Abstrakt

Alkalicko-silikátová reakce (ASR) je reakce charakteristická pro prostředí betonových a maltových konstrukcí obsahujících reaktivní formy $SiO_2$. Za extrémně vysokého pH a dostatečné vlhkosti dochází k rozpouštění $SiO_2$ a ke vzniku alkalicko-křemičitých gelů. Alkalicko-křemičité gely jsou schopny sorbovat molekuly vody, zvětšovat svůj objem a následně způsobit mechanické porušení betonu. Hlavními makroskopickými projevy ASR jsou: bílé nebo průhledné gelovité povlaky (při vysoušení ojediněle tmavnoucí), sítě trhlin a drolení a odpadávání povrchových částí betonu. Způsobem jak zabránit ASR může být vedle chemických přísad do betonu i omezení použití alkalicky reaktivního kameniva. K přesné identifikaci reaktivních forem kameniva jsou zpravidla používány dilatometrické a petrografické metody.

Předložená disertační práce má za cíl propojit petrografické metody, používané geology, s ASR potenciálem kameniva měřeným na experimentálních vzorcích i v přirozeně vzniklých betonových konstrukcích.

Vznik ASR v betonových konstrukcích nacházejících se v České republice, byl zkoumán za použití petrografických metod (optické mikroskopie, petrografické analýzy obrazu a elektronové mikroskopie kombinované s energiově disperzním spektrometrem - SEM/EDS) s cílem určit rozsah poruch způsobených ASR, mikroskopicky identifikovat hlavní projevy ASR a určit hlavní typy alkalicky reaktivního kameniva.

Stejné petrografické metody byly použity ke studiu těženého kameniva (křemenných písků a štěrkopísků těžených v oblastech v okolí řek Cidlina, Dyje, Ohře, Sázava a především v Polabí) a ke studiu experimentálních maltových těles obsahujících stejné vzorky kameniva. Experimentálně stanovený ASR potenciál kameniva tak bylo možné porovnat s petrografickými vlastnostmi kameniva. Zároveň bylo možné pozorovat vznik ASR za experimentálních podmínek a přímo identifikovat reaktivní složky kameniva.

Z maximálně reaktivních forem kameniva byly popsány rohovcem bohaté vápence, představující hlavní složku hrubého kameniva v betonu odebraném ze svodidel dálničního úseku v Praze. Rohovec, velmi jemnozrnná až amorfní forma $SiO_2$, je světově známým typem kameniva s maximální reaktivností. Jeho vysoký stupeň náchylnosti k ASR se v betonu projevuje intenzivní sítí ASR trhlin a dutin, částečně nebo úplně vyplněných alkalicko-křemičitými gely. Jelikož nebyly ve svodidlech pozorovány jiné alkalicky reaktivní složky kameniva, lze předpokládat, že vznik alkalicko-křemičitých gelů v objemu 2,3 - 4,9 obj. % je

způsoben křemičitými vápenci o objemu 4,0 - 7,0 obj. %. Ve vzorcích betonu ze svodidel bylo identifikováno vysoké množství dalších vápencových úlomků (22,0 - 27,4 obj. %). Přesné stanovení podílu křemičité složky ve vápencích je za použití optického mikroskopu značně komplikované a lze proto předpokládat variabilní podíl křemičité složky i v těchto úlomcích, stejně tak jako jejich účast při vzniku alkalicko-křemičitých gelů.

Křemenem bohaté typy kameniva (např. křemenem bohaté sedimentární horniny, metasedimenty a metamorfity) jsou nejrozšířenější skupinou kameniva přítomnou ve vzorcích betonu a zároveň hlavní složkou laboratorně zkoušených křemenných písků a štěrkopísků. Experimentálně byly tyto typy kameniva klasifikovány jako potencionálně reaktivní (resp. středně reaktivní). K upřesnění jejich náchylnosti k ASR přispělo zejména použití petrografických metod při studiu maltových zkušebních těles a petrografický výzkum betonu. Intenzita projevů ASR křemenných typů kameniva do značné míry závisí na stáří vzorků. Maximální stupeň ASR (0,5 - 0,9 obj. % alkalicko-křemičitých gelů a výrazně vyvinutá síť ASR trhlin poškozující cementové pojivo i kamenivo) byly pozorovány ve vzorcích betonu pocházejících z 1. poloviny minulého století. U mladších vzorků betonu stupeň poškození v důsledku ASR klesá.

Velmi malé až nulové projevy ASR byly pozorovány ve spojitosti s některými typy magmatických hornin, obzvláště pak s granitoidy, bazaltoidy a serpentinity. Tyto typy kameniva byly identifikovány ve vzorcích písků a štěrkopísků stejně tak jako v některých vzorcích betonu, kde tvoří hlavní složku hrubého kameniva.

Porovnání projevů ASR v betonu s projevy v maltových tělesech ukázalo na hlavní faktory mající vliv na ASR. Vliv času (stáří vzorků) se projevil v nejstarších vzorcích betonu v podobě částečné "krystalizace" alkalicko-křemičitých gelů. Zároveň lze v betonu pozorovat vyšší intenzitu ASR trhlin. Naopak velmi mladá experimentální maltová tělesa ukazují méně intenzivní porušení v důsledku ASR trhlin ale vyšší podíl alkalicko-křemičitých gelů. Vliv chemismu okolního prostředí (chemické složení cementového pojiva a urychlujících roztoků) se projevuje především v silně proměnlivém poměru $Na_2O$ - $K_2O$ - CaO v alkalicko-křemičitých gelech. Pozorování vzniku trhlin bylo ve všech vzorcích provedeno pouze kvalitativně. V budoucím výzkumu ASR v České republice bude proto nutné této problematice věnovat zvýšenou pozornost.

Druhým tématem, vhodným k intenzivnímu výzkumu v budoucnosti, a částečně otevřeným během této disertační práce je problematika ASR potenciálu křemenem bohatých typů kameniva ve spojitosti s jejich strukturními, deformačními i rekrystalizačními vlastnostmi. Alkalická

reaktivita křemene je celosvětově nedořešeným tématem a v minulosti v České republice řešena nebyla. Vybrané vzorky písků a štěrkopísků, stejně jako vzorky betonu, byly podrobeny detailní analýze strukturně-deformačních, rekrystalizačních a zrnitostních vlastností. Nejvyšší stupeň ASR byl pozorován ve spojitosti s velmi jemnozrnnými křemennými úlomky, ve kterých docházelo během jejich geologického vývoje ke vzniku většího množství několik μm velkých křemenných zrn hromadících se podél staršího hrubozrnného křemene. Tento jev je v literatuře přisuzován rekrystalizačnímu mechanismu bullging, vznikajícímu za nízkých teplot během nedokonalé rekrystalizace. Lépe rekrystalizované křemenné úlomky charakteristické pro výše teplotní rekrystalizační režimy (mechanizmy subgrain rotation a grain boundary migration) obsahují křemenná zrna o vyšším průměru. Jejich ASR potenciál je zároveň nižší. Vzhledem k malému počtu analyzovaných vzorků, je průkaznost vztahu mezi uvedenými petrografickými vlastnostmi a reaktivitou vzorků velmi nízká a je nutné ji ověřit v budoucnosti.

Posledním přínosem této studie je snaha propojit získané výsledky s testování kameniva v praxi. Nově vyvinutá metodika petrografického výzkumu maltových zkušebních těles byla navržena k doplnění do novelizované verze Technického předpisu TP 137 upravujícího zkoušení kameniva a jeho náchylnosti k ASR v České republice.

## Table of contents:

## Appendix:

Appendix A:

Lukschová Š., Přikryl R., Pertold Z. (in print) Petrographic identification of alkali-silica reactive aggregates in concrete from 20th century bridges, Construction and Building Materials.

Appendix B:

Lukschová Š, Přikryl R. (2006): Quantification of Reactive Components in Sands and Gravels by Petrographic Image Analysis (Modified RILEM Method). Proceedings of the 2nd International Conference on Concrete Repair, St Malo, France 2006.

Appendix C:

Lukschová Š, Přikryl R., Pertold Z. (under review) Evaluation of sands alkali-silica reactivity potential: combination of quantitative petrography and dilatometric method. ACI Materials Journal.

Appendix D:

Lukschová Š., Přikryl R., Pertold Z. (2008): Identification of alkali-silica reactive fragments in sands and gravels using mortar bar method and gel pat test, modified by petrographic image analysis. In: Broekmans M.A.T.M., Wigum B. (Eds.): Proceedings of the 13th International Conference on Alkali Aggregate Reaction. Trondheim.

Appendix E:

Lukschová Š., Přikryl R., Pertold Z. (under review) Alkali-silica reaction products: comparison between samples from real concrete structures and from laboratory test specimens. Materials Characterization.

## List of figures:

## List of tables:

# 1. Introduction - alkali-silica reaction

## 1.1. Alkali-silica reaction, its origin and mechanisms

The alkali-silica reaction (ASR) is a heterogeneous solid-liquid reaction, during which alkalis attack the aggregates within concrete. The reaction occurs if the following factors are fulfilled: (1) the presence of alkali reactive aggregates, (2) high alkaline conditions in the cement, and (3) water input. The reaction takes place in open-air concrete structures (*e.g.* dams, roads, highways, and bridges) which are exposed to precipitation. Failures in the drainage system and non-functional waterproofing enable water input into the construction (*e.g.* [1], [2]). Alkaline solution migrates through the pore spaces in the concrete and attacks the aggregates. Hydrated silanol groups formed on the surface of the aggregate (silicates or silica) react with alkaline cations, resulting in the growth of alkali-silica gels. The alkali-silica gels can absorb water molecules, which increase their volume in a manner similar to expandable clays [2]. The internal pressure may exceed the consistency limits of the concrete, leading to mechanical failures of the structures (*e.g.* [2], [3]). Open air cracks, fracturing, and white coatings denote typical macroscopic manifestations of alkali-silica reaction on the concrete surface [4].

## 1.2. Development of ASR investigation

Although first reports on ASR of aggregates been published in the very early part of 20$^{th}$ century [5], the first detailed studies occurred in the 1940s, when Stanton first discussed the formation of alkali-silica gels in a concrete dam in California [6]. The next investigation focused on the alkali-silica reaction mechanisms and the alkali-reactive aggregates (*e.g.* [7]). It was soon recognized that the ASR is not restricted to one aggregate type. It was thus essential to develop methods for the assessment of aggregate vulnerability to ASR (*e.g.* [8], [9], [10]). Fine-grained and amorphous forms of silica were found to be the most reactive components in aggregates (*e.g.* [2]). Medium alkali-silica reactivity potential was determined for volcanic rocks, such as basalts and also for fine-grained metamorphosed quartz-rich rock. Investigation of ASR mechanisms and silica solubility showed that the extent of ASR is not only a function of alkali content in cement, but that it also depends on the ratio between the alkalis and reactive silica (*e.g.* [11]).

Later, extensive research on concrete focused upon the identification of alkali reactive aggregates, descriptions of the ASR mechanism, as well as its products (*e.g.* [8], [12], [13], [14]). By 1991 more than 1300 research papers dealing with ASR had been published [15].

During the last two decades ASR research had split into the following topics: ASR mechanisms (*e.g.* [16], [17]), investigation of alkali reactive aggregates (*e.g.* [18], [19], [20]), determination and prediction of the ASR potential of aggregates (*e.g.* [21] - [27]), the macroscopic and microscopic identification of ASR in concrete (*e.g.* [4], [28] - [31]), and the mitigation of ASR (*e.g.* [32] - [35]).

Petrographic methods had become widely applied to the investigation of concrete samples during the 1980s and 1990s (*e.g.* [2], [36]). These methods facilitated identification of the mechanisms of damage in concrete, *e.g.* sulphate attack [37], frost, fire damage [38 - 40], delayed ettringite formation [41, 42], and steel corrosion [43]. Both optical microscopy and electron microscopy, combined with energy dispersive spectrometry, contributed significantly to the understanding of concrete ASR damage on the microscale (*e.g.* [29], [44 - 49]). However, common optical microscopy has rarely been applied, except to the detailed crack mapping (*e.g.* [50]) and cement paste investigations.

## 1.3. Investigation of ASR in the Czech Republic

In the Czech Republic, petrographic research of ASR in concrete was first investigated in the 1990s due to extensive damage of highway D-11 from Prague to Poděbrady. Concrete decay was attributed to the use of aggregate (both crushed and natural) containing a high percentage of particles composed of reactive forms of silica [51]. This case initiated interdisciplinary research conducted at the Klokner Institute at the Czech Technical University in Prague, during which different aggregates including igneous, metamorphic, and sedimentary rocks were tested [52]. Petrographic methods (optical microscopy) were only applied to determine the mineralogical composition of the aggregates. Alkali-silica reactivity potential of the tested rock types was measured according to the expansion values of mortar bar specimens (following the standards ASTM C1260 [53], DafStb [54], RILEM AAR-1 [55] and ČSN 72 1179 [56]), and also according to the soluble $SiO_2$ content as well as alkalinity reduction (both following standard ČSN 72 1178 [57]). This research led to the establishment of a database including: the tested rock types, their localities, and their ASR potential (as well as a database of cements used in the Czech Republic with their chemical composition and $Na_2O_{ekv}$ values). Czech standards ČSN

721179 [56], ČSN 72 1153 [58], and ČSN 72 1180 [59] were updated by the inclusion of selected international standards. The final summary was published as the Czech technical regulation TP 137 [60], the first Czech regulation specifying ASR in concrete and its petrographic investigation [52].

In current practice, the rocks used as filler in concrete are evaluated by the technical regulation, mentioned above (TP 137 [60]). This technical regulation specifies the requirements for the cement paste and for the preparation of concrete including admixtures; plus, it regulates the use of other Czech standards (*e.g.* [56], [58], [59]) with respect to their applicability for the testing of aggregate ASR vulnerability. Required test methods for aggregates include (a) petrographic analysis of aggregates following the ČSN 72 1153 standard [58]; (b) chemical analysis of aggregates, following the ČSN 72 1178 and ČSN 72 1179 standards [56,57]; (c) detailed petrographic identification of aggregates classified as reactive in ASR, listed in TP 137, following the ČSN 72 1180 standard [59]; (d) the dilatometric method, following the ČSN 72 1179 standard [56]; (e) the accelerated dilatometric method, following the ASTM C1260 test method [53]; and (f) the dilatometric method, following the ČSN 72 1160 [61] standard, to identify alkali-carbonate reactive aggregates. Additionally, regulation TP 137 [60] declares the ASR to be open for further investigation.

## 1.4. Aims of the research

The alkali silica reaction in concrete has been underestimated in the Czech Republic for a long time, although it might well lead to the ultimate destruction of various concrete building blocks. Therefore, it is crucial to understand this reaction properly, so one can remove it from engineering materials completely or at least suppress its action in a satisfactory manner. Despite the fact that it was recognized as early as the 1990s, the idea that it was important to know the alkali-silica reactivity of the concrete's components (if one wants to avoid damage of the concrete) was still missing; as was any detailed study that would deal with Czech aggregates. In addition, there exist plenty ample modern techniques that can be implemented for evaluation of ASR, but surprisingly have not yet been used in practice. That inspired us to develop and/or update suitable petrographic, dilational, and chemical methods with the intent that they could be applicable in practice, and suitable for the complex characterization of aggregates with respect to their ASR potential.

In particular, this PhD thesis aims at:

- Testing the applicability of petrographic techniques to real concrete structures, to experimental specimens whose composition has been restricted by the uniform composition of cement paste, and by the choice of different types of aggregates.
- Observing ASR reactivity with respect to the surrounding conditions and the type of alkali reactive aggregates. To fulfil this task, we investigated both real samples and experimental specimens (which have the great advantage, compared to real samples, that one can more easily control external factors influencing the ASR reactivity).
- Developing/updating methods suitable for testing of ASR potential, in practice, such as mortar bar and petrographic methods.
- Investigating concrete constructions possibly affected by ASR, and to find-out whether the ASR had really been the source of the damage or not. If it was the case, then we wanted to know what induced the reaction to proceed in the samples. The concrete constructions had been carefully chosen by the Czech Directorate of Highways and Motorways, who are greatly interested to avoid ASR in future constructions, ranging from highways to roads, dams and bridges in the Czech Republic.
- Addressing the problem of the ASR potential of quartz-rich aggregates (widely used in concrete industry due to their low cost). The ASR potential of these aggregates is strongly dependent on the type, composition and geologic history of aggregates. The commonly used explanation of their ASR potential, being based upon the angle of undulatory extinction, is unsatisfactory and needs more detailed investigation.

The PhD thesis is divided into two parts: the main text, and amendments. The main text of the thesis (Sections 1 – 6) comprises the investigation of concrete bridges and crash barrier; summarises the testing the quartz-rich sands and gravels and the determination of their ASR potential; and discusses the manifestations of ASR. The amendments (Appendix A - Appendix E) represent results previously published in various papers (sent and/or revised) in five different international journals or conference proceedings. The main text's objective is to give a comprehensive overview of the investigation carried-out. Unpublished results are discussed in detail. Those conclusions, summarised within previous papers, are discussed briefly and referenced to the original papers (in Appendix A - Appendix E).

# 2. Identification of alkali-silica reaction in real concrete structures

## 2.1. Overview of the methods used in concrete petrography

The use of petrographic examinations of concrete and mortar was mainly influenced by the development of microscopic techniques. The polarising microscope (constructed by A. Nachet in Paris in 1857) was originally designed as a chemical microscope for the examination of crystals. During the next two or three decades, polarising microscopes were adopted by mineralogists and became the most important method used in geology-related subjects [2].

Early scientists soon established the importance of the petrographic microscope for the investigation of artificial inorganic materials; however, they were limited by the resolution properties of microscopes [62, 63]. The petrographic examination of concrete and mortar materials developed more rapidly during the 1960s, when large-area thin-sections became available. Since then, concrete petrography has frequently been used for the identification of concrete and mortar components, for the identification of cement paste phases, and especially for the identification of concrete and mortar degradation mechanisms (*e.g.* [2, 38, 64]).

The latest case involves numerous methods, working on both the macro- and microscale. *In situ* inspection of concrete constructions influences the quality of all further steps of successive investigations. It enables discrimination of macroscopically visible cracks (Fig.1) and white coatings on the concrete surface, the most important macroscopic indicators of ASR (*e.g.* [28], [30]). The quantitative measurement of the length of macrocracks seems to be an effective indicator of the structural integrity of concrete [48]. A direct correlation between ASR signs (length of microcracks) and the deterioration of concrete's mechanical properties, however, has not been confirmed [65].

Macroscopic laboratory identification of ASR in concrete samples is conducted using both the uranyl acetate method and colouring methods (*e.g.* [66 - 69]). Optical microscopy and SEM/EDS enable the identification of phases in the cement paste (*e.g.* [70]), petrographic classification of aggregates, investigation of damaging mechanisms, and a determination of modal composition (*e.g.* [4], [29], [71]). Combined study by SEM/EDS and X-ray diffraction analysis (XRD) explores the maturation and crystallization of alkali-silica gels [30, 72].

ASR is commonly confused for the alkali-carbonate reaction (ACR), principally if only macroscopic observation is conducted (*e.g.* [73 - 76]). Both reactions (ASR and ACR) cause the expansion of concrete and macroscopically visible cracks. Alkali-silica gels, forming white coatings on the concrete surface are only characteristic of ASR, but they do not necessarily accompany all ASR situations.

The mechanism of ACR remains unexplained, although the mechanism of dolomite replacement by brucite and calcite is favoured by numerous authors (*e.g.* [73], [77]). Growth of brucite crystals is probably responsible for expansion in concrete, due to its crystallization pressure [77]. On the macroscale, the replacement of dolomite by brucite and calcite is hardly visible, and ACR cannot be recognised.

The other important fact, contributing to ASR - ACR confusion, is associated with the presence of very fine-grained silica in dolomitic limestone. Without detailed microscopic investigation, the fine-grained silica is not likely to be detected. Thus, there was an open question about the alkali-carbonate reaction's existence, or its possible confusion for ASR [73, 77].

## 2.2. Petrographic methods applied to the investigation of real concrete structures

### 2.2.1. In situ macroscopic observation of ASR

*In-situ* inspection of concrete constructions represents the crucial point in the investigation of damaging mechanisms. The surface exposure of concrete degradation may indicate the type of degradation. (*e.g.* steel corrosion in concrete is mainly manifested by brown or reddish-brown coatings on the surface, [36, 78]).

Some concrete degradation mechanisms are exhibited in a similar manner. The crack network is characteristic for freeze/thaw disintegration, as well as for ASR or ACR. In this case, *in-situ* inspection is regarded as the initial point of an investigation, providing selection of the sampling points [2, 36].

In 2006, concrete bridges (constructed between 1924 - 2000) were inspected at various localities in the Czech Republic. *In-situ* inspection showed in-leak into the construction joints, deep concrete degradation, and steel corrosion in 13 of the inspected structures [79, 80]. In 2007, a

network of cracks was observed also covering a crash barrier (constructed in 2000) located in Prague (see Fig. 1) [81, 82]. The most important macroscopic signs of ASR, a network of cracks, were detected to a variable extent in all of the sampled structures. Because macroscopically detected ASR cracks can be confused for the freeze/thaw disintegration or delayed ettringite formation (St John *et al.* 1998, Sahu and Thaulow 2004), a laboratory examination of concrete samples was required (see Appendix A).

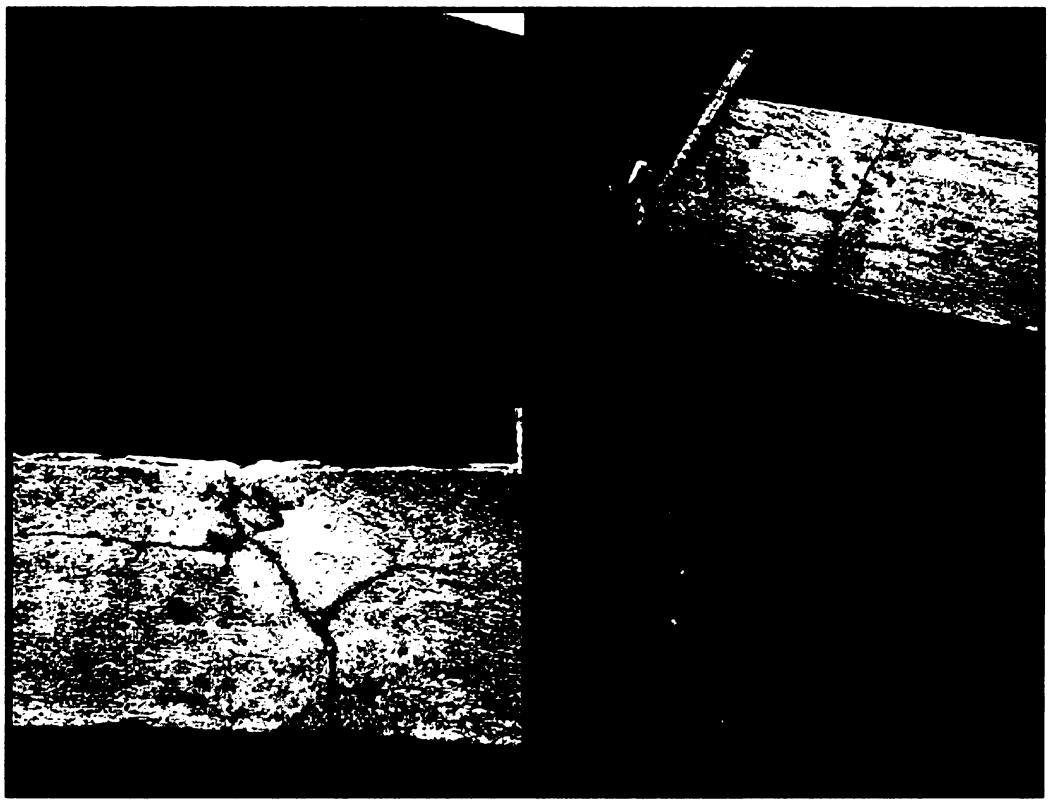

Figure 1. *In situ* inspection of ASR in a concrete crash barrier - vertical side (a), horizontal (surface) side (b, c), detailed view on ASR cracks (c, d) (adopted from [83], modified).

Cracks covering the concrete surface exhibited shape, position, and branching characteristic for ASR. Cracks are well developed in areas with higher inputs of water (joints with non-functioning waterproofing) and intrude into the concrete's interior. Macroscopically invisible termination of these cracks is discernible by a differing coloured area, without open fracture. White or glassy coatings of alkali-silica gels are occasionally visible.

Cracks intruding aggregates are more detectable, macroscopically, and associated with colour differentiation in the surrounding area (Fig. 2, part a). All macroscopic features described above are characteristic for ASR (*e.g.* [2], [29]).

### 2.2.2. Laboratory macroscopic identification of ASR

Laboratory macroscopic examination provides identification of any unusual features, as well as a description of the general characteristics of the samples. Surface discolouration and the presence of cracks and alkali-silica gels could be observed visually or by using laboratory colouring and fluorescent methods. Fluorescent epoxy dyes are applied, especially in the determination of the volume of pore voids (*e.g.* [2, 4, 28]). Both colouring and uranyl acetate agents are used to point-out the characteristic signs of ASR (*e.g.* [2]).

The uranyl acetate solution is sprayed on a washed concrete surface. After a few minutes, the uranyl acetate is absorbed by the alkali-silica gels, the characteristic products of ASR. The concrete surface is observed and photographed under ultraviolet light, at 240 nm. Alkali-silica gels absorbing the uranyl acetate show-up as a green or yellowish-green colour [66, 69].

In the first half of 20$^{th}$ century, the reaction between Rhodamine B and $Ca^{2+}$ cations, as well as between sodium cobalt nitride and $K^+$ cations was used for the identification of $K^+$ and $Ca^{2+}$ rich feldspars. These colouring agents facilitate identification of $Ca^{2+}$ and $K^+$ rich silica gels [67, 68]. $Ca^{2+}$ rich silica gels stained pink and $K^+$ rich silica gels stain a yellow colour.

The uranyl acetate method was applied on concrete samples from the crash barrier (as a part of the initial investigation of concrete samples, conducted by Horský Ltd.), showing intensive concrete degradation. Intensively yellow or yellowish-green cracks were observed surrounding aggregates, and intruding aggregates and the cement paste (see Fig.2, part b) [83].

The colouring agents Rhodamine B and sodium cobalt nitride were applied with the objective being to macroscopically identify alkali-silica gels in the concrete samples, investigated as a part of this study. Concrete samples were cut into 1 - 2 cm thin slabs. The slab size was restricted only by the size of laboratory equipment used during the colouring procedure. Concrete slabs were put into glass containers with the dissolved colouring agents. The colouring periods varied between 24 hours for sodium cobalt nitride to 1 - 10 minutes for Rhodamine B.

Both yellow and pink areas were observed in the concrete samples after the staining procedure. These features could be partially explained by the presence of alkali-silica gels, and partially by their association with other factors:

- The intensive pink and yellow colours of some fragments in the concrete samples indicate the presence of $K^+$ and $Ca^{2+}$ rich feldspars.

- Large pink coloured areas in the concrete samples reflected high content of $Ca^{2+}$ ions in the cement paste, and can be caused by an increasing volume of alkali-silica gels in the cement paste. A similar explanation could be established for weakly coloured yellow areas of cement paste. These features can barely be distinguished by macroscopic observation.
- Intensively coloured pink rims surrounding the aggregates indicate the presence of alkali-silica gels filling the cracks between the aggregate and cement paste (Fig.3).
- Cracks (crack patterns) highlighted by pink and yellow colour, intruding the cement paste and aggregates, indicate the ASR cracks (Fig.3).

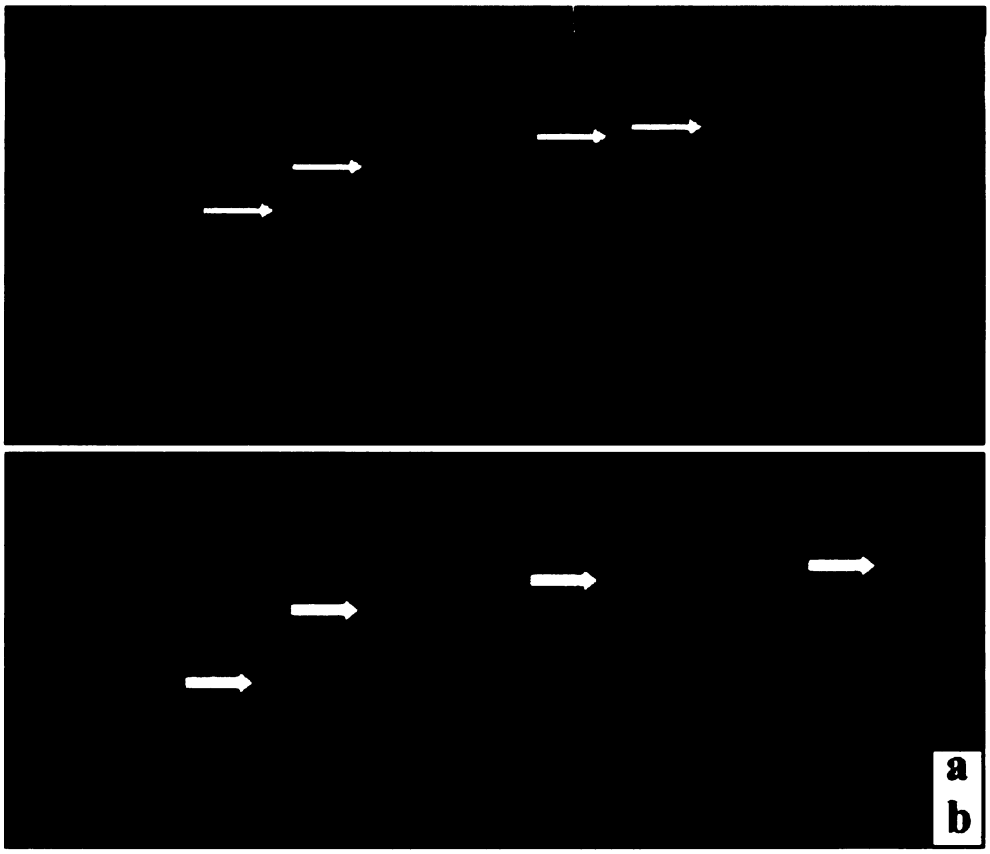


Figure 2, part a. Concrete drill core no. V4 (taken from crash barrier, constructed in 2000). White arrows indicate positions of ASR cracks (adopted from [83], modified). (part b) Concrete drill core impregnated by uranyl acetate. Yellow rims surrounding aggregates show positions of the alkali-silica gels (indicated by white arrows, photograph taken from the same concrete drill core as in part a, adopted from [83], modified).

The above-mentioned conclusions, concerning the colouring methods applied on concrete samples, were checked and confirmed by both optical and electron microscopy (discussed in Appendix A). Based on the laboratory macroscopic investigation, colouring agents were accepted as possible indicators of ASR in concrete; facilitating selection of areas from which

thin sections were to be prepared. Possible confusion of colouring associated with ASR, to colouring associated with other features, suggests the application of colouring methods only in the initial stage of concrete investigation. Confirmation of the presence of ASR, and its detailed investigation, can only be performed by microscopic investigation.


Figure 3. Colouring methods using sodium cobalt nitride (part a-b) and Rhodamine B (part c). Intensive yellow coloured areas in parts a and b (*viz.* pink coloured areas in part c) reflect the possible presence of alkali-silica gels. Concrete sample no. 232-007 (from Liblín, constructed in 1929, part a, b) and concrete sample no. 610-018 (from Stará Boleslav, constructed in 1982, part c).

### 2.2.3. Microscopic identification of ASR

Optical microscopy, petrographic image analysis, and SEM/EDS method represent the fundamental techniques used in the investigation of artificial materials such as clinker, cement, grout, mortar, and concrete. Microscopic techniques coupled with chemical analysis, X-ray diffraction and/or DTA analysis comprise effective means to study cement's raw materials, burning history, and the phase relationship of clinker. The petrographic microscope is used to study the spatial relationship between individual components in artificial materials. The final advantage of the petrographic microscope is its preferred use in the identification of the degradation mechanisms in concrete, including ASR (*e.g.* [2, 29, 31, 45, 47]).

Numerous microscopic signs of ASR in concrete are influenced by the extent of the reaction, size and distribution of the reacting aggregates, distribution of pore voids, as well as chemical composition and structure of the cement paste. The ASR in concrete is discernible by the following features: alkali-silica gels, ASR cracks, and aggregates affected by ASR [2].

Detailed microscopic investigations of the studied concrete samples, taken from bridge constructions, are to be found in Appendix A. A preliminary microscopic investigation of

concrete samples taken from the crash barrier (conducted by Pauliš Ltd.) showed no signs of ASR. Coarse aggregates were described as limestones, unaffected by ASR. Also, no signs of ASR were described in connection with fine aggregates composed of quartz fragments [83].

An independent investigation of ASR features, conducted as a part of this thesis, involved a laboratory macroscopic investigation using colouring agents (Rhodamine B and sodium cobalt nitride) and microscopic methods (optical microscopy, petrographic image analysis and SEM/EDS). All experimental methods are similar to those applied as a part of the investigation of concrete sampled from bridge constructions (see Appendix A). The degree of ASR reaction can be determined according to the intensity of ASR signs, and divided into the four following subgroups:

- Concrete unaffected by ASR - characteristic of concrete samples composed of non-reactive aggregates (*e.g.* diabase, granitoid, serpenite and olivinic basaltoide rock fragments), without any effect of the time factor. No microscopic signs of ASR were detected in the samples. Thus *in-situ* observed concrete degradation is caused by other degradation mechanisms (*e.g.* freezing-thawing) (*e.g.* concrete samples no. 14-070, 14-071 and/or 1 - 2 from Trutnov and Mirotice).
- Concrete slightly affected by ASR - mainly characteristic of the early stages of ASR in concrete, containing slowly reactive aggregates composed of quartz aggregates and meta-greywacke. In these stages, ASR can barely be identified, according to macroscopic signs. *In-situ* observed degradation could be explained by other mechanisms. Microscopic signs of ASR are just barely detectable. Aggregates are unaffected by ASR cracks. The volume of alkali-silica gels is very low (*e.g.* concrete sample no. 610-018 from Stará Boleslav, constructed in 1978). Future increases of ASR in concrete construction is to be expected.
- Concrete with a medium degree of ASR is characterised by the middle or late stage of ASR, and is composed of alkali-reactive aggregates such as quartz aggregates or quartzite. The aggregates, in combination with long exposure periods (in many cases greater than 50 years), caused a well-developed ASR, showing all the characteristic signs. Alkali-silica gels are present in pore voids, in cement paste and especially filling the cracks intruding aggregates. Cracks are isolated (intruding one aggregate) or interconnected, forming networks intruding more than one aggregate, as well as the cement paste (*e.g.* samples no. 180-010, 232-007, 272-006 from Dolany, Liblín and Lysá nad Labem). The well-developed system of cracks, partially filled by alkali-silica gels, is conventionally accepted as a direct indicator of ASR (*e.g.* [2, 36, 45, 65]).
- Concrete highly affected by ASR is characterised by an extensive ASR crack network observed both on the macro- and microscale. Alkali-silica gels are discernible by a

white or transparent coating on the concrete surface. On the micro-scale, there is visible a high volume of alkali-silica gels (exceeding 1.0 vol. %), occasionally situated in the "split" form. This degree of ASR was observed in connection with concrete samples composed of chert-rich limestones, well known in the literature as highly reactive (*e.g.* [75, 76]).

### 2.2.4. Modal composition of bulk concrete structures: benefits of petrographic image analysis

The employment of petrographic image analysis was verified in different applications, such as: the determination of modal composition of natural and artificial samples, investigation of structural and textural parameters of aggregates, and investigation of the degree of deterioration in concrete and mortars. Petrographic image analysis is a computer-assisted method which enables one to measure point, linear, and planar objects in digital images. Projection of 3D objects into 2D enables one to characterise bulk samples (*e.g.* [84, 85, 86]).

Petrographic image analysis is the most satisfactory technique to determine the modal composition of samples, based upon the determination of modal composition of thin sections, prepared from studied samples (*e.g.* [65, 84, 87]). In the investigation of concrete, the petrographic image analysis was successfully applied in the determination of the cement paste / pore voids ratio, the petrographic characteristic of aggregates and cement phase; as well as in the investigation of fire damage in concrete, steel corrosion, and/or other degradation mechanisms (*e.g.* [38, 41, 42, 78]).

In the case of studied concrete samples, petrographic image analysis enables one to determine the petrographic characteristics of aggregates, as well as the modal composition of bulk concrete samples. The most important advantage is seen in the investigation of the spatial distribution of aggregates: pore voids, cement paste, and newly formed alkali-silica gels (see Appendix A).

The modal composition of concrete samples from the crash barrier was comparable with samples from the bridge constructions. The main components are the following: fine aggregates (aggregates with a diameter less than 4 mm), coarse aggregates (aggregates with a diameter greater than 4 mm), cement paste, and pore voids. Pore voids are characterised by circular or amoeboid shapes. They are frequently filled by alkali-silica gels or (rarely) are empty (filled only by epoxy dye). The pore size varies between 0.1 mm (predominantly in the case of circular

pores) and 8.2 mm (predominantly in the case of amoeboid pores); rarely, they can be larger or interconnected with other pores or with cracks.

Four main differences are seen in the comparison of concrete samples from a crash barrier with those from bridge constructions:

- The volume of pore voids, counted together with the volume of ASR cracks, was higher in the concrete crash barrier (varying between 5.2 - 8.7 vol. %). The largest volume of pore voids and cracks identified in the concrete samples, coincided with the most intensively damaged by ASR (see detailed discussion below).
- The volume of cement paste in the concrete samples varies between 44.4 - 47.7 vol. %, showing less variability, compared with the volume of cement paste calculated in concrete samples from bridge constructions (varying between 32.7 and 52.3 vol. %, mentioned in Tab. 2 in Appendix A). The smaller variability of cement paste volume, in the case of concrete samples from a crash barrier, could be explained by the uniform conditions during mixing and preparation of the concrete in the crash barrier. Due to the different positions, and dates of bridge constructions, one can assume different conditions in the preparations of the cement pastes and concretes.
- Lesser variability is also seen in the volume proportion of coarse and fine aggregates and in their petrographic composition (sees Tab. 1 and 2). Fine aggregates in concrete sampled from a crash barrier are composed of quartz fragments and their volume varies from between 12.0 and 16.4 vol. % (Tab. 1). The volume of fine aggregates in concrete sampled from bridge constructions, composed of quartz, feldspar, mica, phyllite, and granitoid fragments varies between 13.5 and 26.4 vol. % (see Tab. 2 in Appendix A).
- The uniform composition and modal ratio of coarse aggregates from the concrete crash barrier (Tab. 1, 2), composed of limestone and chert-rich limestone, contrasts with the volume and petrographic variability of coarse aggregates from the concrete bridges, with a higher variability of between 22.8 and 51.1 vol. % (Tab. 2 in Appendix A). They are composed of variable rock types of magmatic (diabase, basaltoide, olivinic basaltoide, serpentinite, diorite, granite), metamorphic (meta-greywacke, gneiss etc.), and sedimentary (quartzite, pelite, limestone etc.) origins (Tab. 3 in Appendix A).
- The volume of alkali-silica gels and ASR cracks is higher and more variable in the concrete crash barrier, when contrasted with the bridge constructions. This observation cannot be explained by the dates of construction of the concrete bridges (see Appendix A). The ASR caused by quartz and quartzite aggregates in concrete strongly depends on the age of the concrete construction. The quartz aggregates, as well as meta-sedimentary and sedimentary rocks, containing a high amount of deformed quartz, are slowly reactive; and the ASR can originate after 10 years, 20 years, or longer periods [26, 47,

88]. In contrast, the concrete crash barrier shows a high amount of alkali-silica gels and extensive crack networks 7 years after its construction.

All features mentioned above were caused by uniform concrete mixtures and the use of aggregates exploited from the same quarries in the case of the concrete crash barrier, in contrast with the different bridge constructions.

Table 1. Proportion of the main components of concrete samples as determined by petrographic image analysis. All data in vol. %, n.d. – not determined. All samples (samples no. V6, V9, and V11) were taken from concrete crash barrier located in Prague (constructed in 2000).

| Sample n. | Coarse aggregate | Fine aggregate | Cement paste | Voids and cracks | Alkali-silica gels | Total |
|---|---|---|---|---|---|---|
| v6 | 28.9 | 12.0 | 47.3 | 6.9 | 4.9 | 100.0 |
| v9 | 31.4 | 16.4 | 44.7 | 5.2 | 2.3 | 100.0 |
| V11 | 30.7 | 13.1 | 44.4 | 8.7 | 3.1 | 100.0 |

Table 2. Composition of coarse aggregates in concrete samples as determined by petrographic image analysis. All data in vol. %, n.d. – not determined. All samples (sample no. V6, V9, and V11) were taken from concrete crash barrier located in Prague (constructed in 2000).

| Sample n. | Carbonate | Chert-rich limestone |
|---|---|---|
| v6 | 22.0 | 7.0 |
| v9 | 27.4 | 4.0 |
| V11 | 26.1 | 4.6 |

The high degree of ASR and the variable volume of alkali-silica gel in the concrete crash barrier can likely only be explained by the composition of the coarse aggregates. Limestone aggregates (classified as chert-rich aggregates) contain a significant volume of very fine-grained silica (chert). The high ASR potential of chert-rich (siliceous) limestones is well known and established, as well as the fact that the ASR of chert starts rapidly within a few months or years) [75, 76]. A relationship was found between the volume content of chert-rich limestone and the volume of alkali-silica gels, as well as ASR cracks (Fig. 4). This correlation confirms the fact that the ASR in the concrete crash barrier is mainly attributable to the chert-rich limestones.

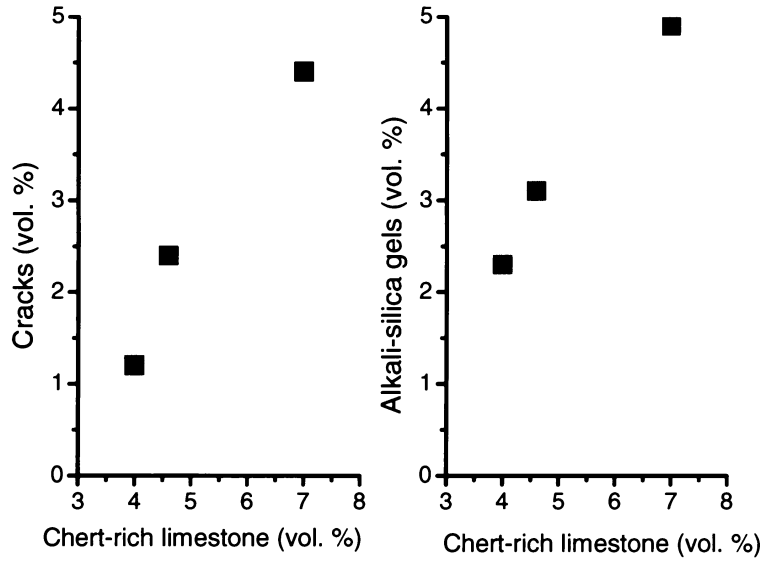


Figure 4. Comparison of the total volume of chert/rich limestone with the volume of cracks (a) and the volume of alkali silica gels (b) in concrete samples from concrete crash barrier (concrete samples no. V6, V9-1, V11 from Prague, constructed in 2000).

## 2.3. Mode of occurrence of the ASR

Alkali-silica gel is the main indication of ASR in concrete, visible on the concrete surface macroscopically, and possible to identify using variable petrographic methods (*e.g.* [2]). The most commonly used, optical and electron microscopy, enable one to distinguish alkali-silica gels from other concrete components, according to their morphology and chemical composition (possible to determine using SEM/EDS method, [29, 45]). Alkali-silica gels are amorphous hydrated alkaline-rich silica phases. Using parallel nicols, alkali-silica gels are colourless with contrasting boundaries (Fig. 5, part a). Using crossed nicols, their colour changes to black, dark brown or reddish dark brown (Fig. 5, part b). Their colour is unchanged in connection with their orientation. The amorphous structure and amoebic boundaries enable one to distinguish them from bubbles and pore voids.

The volume amount of alkali-silica gels, determined using petrographic image analysis as a part of the determination of modal composition of concrete samples, varies between 0.1 vol. % (for the least damaged concrete samples) to 4.5 (for the most damaged). The volume of alkali-silica gels was also compared with the amounts of the aggregates. The highest correlation factor was

found between the volume of alkali-silica gels and the volume of quartzite aggregates (see Fig. 8 in Appendix A).

The volume of alkali-silica gels correlates well with the year of construction (Fig. 6). The following categories of samples were distinguished:

a) Samples containing dominant chert-rich limestones (Group 1), of coarse aggregate. The volume of alkali-silica gels reaches the highest values (over 4.0 vol. %). The influence of the time factor was not evaluated, due to the same year of construction for all samples.

b) Another group of samples containing mostly quartzite, quartz aggregates and meta-greywacke as a major compound of coarse aggregates (Group 2). The volume of alkali-silica gels varies between 0.3 - 0.9 vol. percent, and is strongly dependent on the age of construction.

c) A group of samples containing non-reactive aggregates (*e.g.* diabase, basaltoids, serpentinite, granite and granodiorite) (Group 3). Alkali-silica gels seem to be unaffected by the time factor, reaching a maximum of 0.1 vol. % .

Other signs of ASR, especially characteristic of concrete samples, are cracks intruding the aggregates and cement paste, and communicating with the pore voids. In some cases, cracks form networks passing through the entire sample.

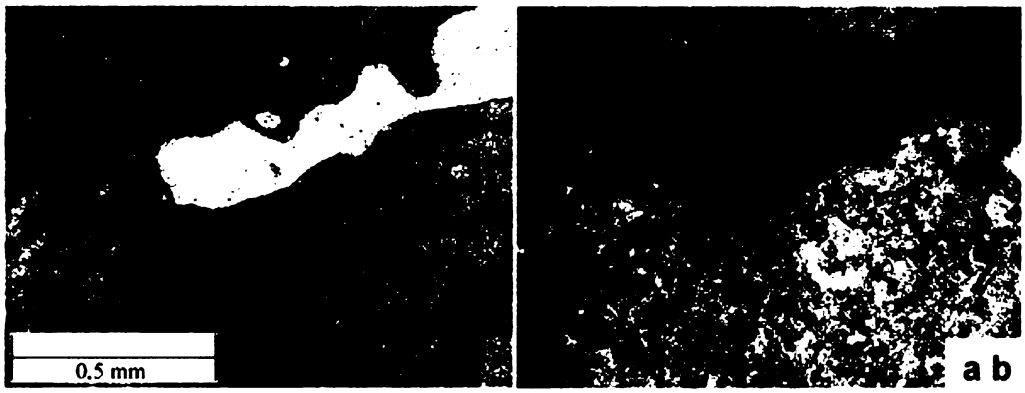


Figure 5. Alkali-silica gel filling the aggregate - cement paste boundary. Optical microscope, parallel (part a) and crossed (part b) nicols, concrete sample no. V4 from crash barrier, Prague. Part b – cement paste (black), alkali-silica gel (brown), chert-rich limestone (blue, yellow, grey and brown).

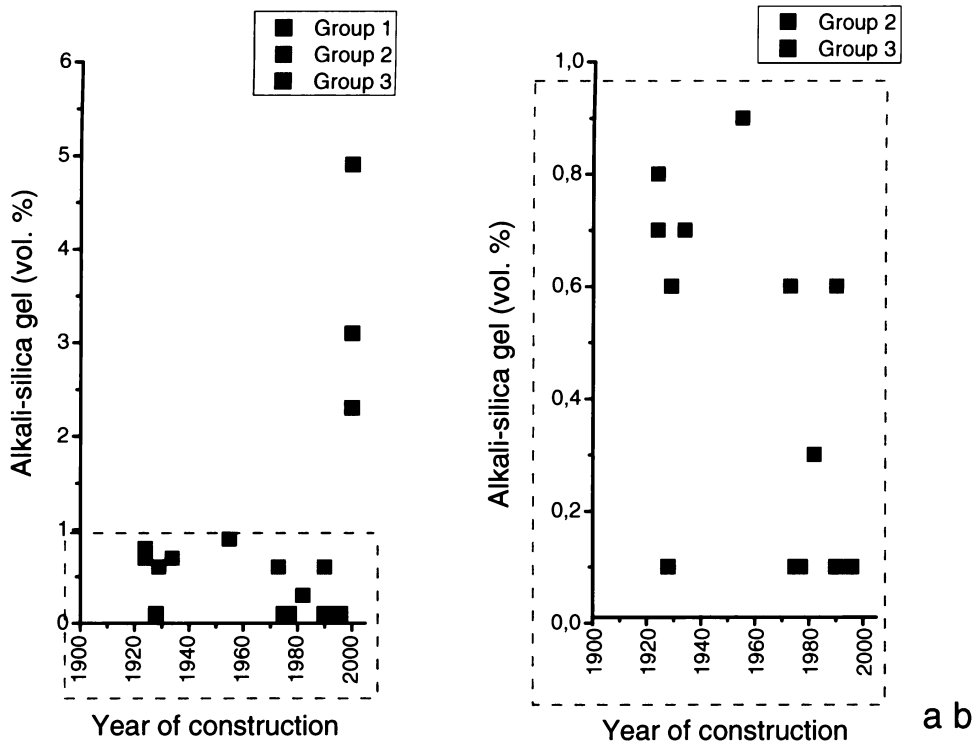


Figure 6. Comparison of volume of alkali-silica gels with the year of construction (adopted from Appendix A and modified). Group 1 - concrete samples containing chert-rich limestone (samples no. V4, V9-1 and V11), Group 2 - concrete samples containing slowly reactive aggregates such as quartzite, meta-greywacke and quartz aggregates (samples no. 180-010, 232-007, 272-007, 610-018, 610-019, 610-035, X604, and MK7), Group 3 - concrete samples containing non reactive aggregates such as granitoids, basaltic rocks and serpentinite (samples no. 14-070, 14-071, DB102, Y531, 1-2, and 2-3).

## 2.4. Influence of silica form

Minimal or no ASR signs were identified in those concrete samples containing granite, granodiorite, serpentinite, and basaltoids in coarse aggregates. Alkali-silica gels form only 0.1 vol. % (which is very close to the detection limit of petrographic image analysis - of about 0.05 vol. %) [84]. Alkali-silica gels were seldom described filling the pore voids. No other signs of ASR were observed in these concrete samples. The low ASR potential of granite, granodiorite and serpentinite is well known [26, 47, 71, 86]. The petrographic methods were used to determine the alkali-silica reactivity potential of aggregates and classify them as non reactive or very low reactive (*e.g.* RILEM AAR-1). Shayan [90] discussed the alkali-silica reactivity of deformed granitic aggregates, in which significant expansion was measured. The ASR was related to microcrystalline quartz accumulating along well-crystallized large quartz grains. The

low alkali-silica reactivity of some plutonic rocks was confirmed by Modrý *et al.* [52] for some Czech granitoid rock types.

Chert-rich limestone was assessed to be the most reactive type of aggregate observed in the concrete samples. Its variable volume (4.0 -7.0 vol. %) caused the 2.3 - 4.9 vol. % of the alkali-silica gels in the 7-year old concrete samples. Other alkali-silica reactive aggregates were observed in these samples, in minimal amounts. Thus, chert-rich aggregates were classified as alkali reactive, with the rapid onset of ASR. This behaviour of limestones and carbonates, rich in fine-grained silica, is well known and widely discussed in recent literature, in connection with ACR. The rapid ASR of fine-grained forms of silica is caused mainly by grain size, specific volume parameters, and amorphous form [73 - 76, 91]; and sometimes can generate a false identification of ACR in concrete, where ASR also originates [73, 75].

Quartz rich aggregates (*e.g.* quartzite, deformed quartz aggregate, meta-greywacke) were identified in 12 out of 17 studied concrete samples. Volume of alkali-silica gels varied between 0.3 - 0.9 vol. % in 8 samples. The strongest influence of quartzite and deformed quartz aggregates on the origin of alkali-silica gels is observable in older concrete samples (samples from the 1$^{st}$ half of 20$^{th}$ century), in which the volume of alkali-silica gels reaches 0.9 vol. %. The slow formation of ASR in quartz-rich aggregates is affected by grain size and deformation parameters. The most extensive and rapid reaction occurs if fine-grained quartzite aggregate is present; while the slowest progress is due to deformed coarse-grained well-crystallized quartz [26, 48, 90].

The ASR potential of well crystallized quartz-rich aggregates is traditionally evaluated by the angle of undulatory extinction (*e.g.* [55]). However, numerous studies have argued for the limited applicability of this single measurement to encompass the complexity of the ASR problem [92, 93]. Some recent studies have shown that the reactivity of crystalline quartz can be more confidently assessed by a detailed examination of the deformation characteristics and grain size of the quartz fragments [18, 20, 26, 27]. A detailed investigation of deformation and recrystallization characteristics in quartz-rich aggregates in concrete samples is compared with a similar investigation applied to experimental mortar specimens and is discussed below (see Section 3.6.2).

## 2.5. Correlation between macroscopic and microscopic signs of ASR

The ASR was identified in studied concrete samples using three different methodology groups:

I. *In-situ* inspection - ASR was observed in all investigated structures, exhibited by a network of cracks covering the concrete surface in variable intensities. Other construction damage, identified in concrete constructions (*e.g.* in-leak into construction joints, concrete surface moulding and crushing, corrosion of steel reinforcement, and leaching of cement paste) contributed to increasing inputs of moisture into the concrete, causing an increasing degree of ASR.

II. Laboratory macroscopic methods - colouring agents (Rhodamine B and sodium cobalt nitride) plus the uranyl acetate method enabled and facilitated the macroscopic identification of ASR in concrete drill cores.

III. Laboratory microscopic methods - provided detailed investigation of individual phases, as well as the determination of the modal composition of concrete samples. Both optical and electron microscopy are regarded as the most important methods in the identification of ASR products. The ASR was confirmed microscopically in 11 of 17 concrete samples, predominantly related to coarse aggregates composed of chert-rich limestone, quartzite, quartz aggregates, metapellite, and meta-greywacke.

The quantitative comparison of macroscopic and microscopic signs of ASR (summarised in Table 3) is impossible, due to the absence of quantification of the macroscopic signs of ASR. This type of quantification is rarely used in world literature, due to the large requirements connected with both systematic and precise photo-documentation, and the process of quantification [48]. Up through 2008, this method had not been included in Czech inspection guides [60].

## 2.6. Summary

Two different groups of methods, macroscopic and microscopic, were applied to concrete samples with the aim to identify the ASR, with differing results. *In situ* observation indicated possible ASR in all investigated structures. In contrast, microscopic methods confirmed the ASR degradation in only 11 out of 14 concrete samples. Thus, macroscopic observation of concrete damage *in situ* is recognized to be insufficient.

The surface concrete damage can reflect different degradation mechanisms (*e.g.* steel reinforcement corrosion and cement paste leaching). The problematic comparison of

macroscopic and microscopic damage in concrete shows the importance of quantitative determination of surface concrete damage, which is absent in this investigation. On the other hand, it supports the importance of petrographic and microscopic methods in concrete investigations.

The microscopic methods and petrographic image analysis were successfully applied in the identification of ASR in concrete, as well as in the petrographic classification and description of aggregates. The main ASR products (alkali-silica gels) fill cracks and pore voids. The ASR cracks intrude aggregates and aggregate-cement paste boundaries. Occasionally, they form a network, interconnecting individual parts of the concrete. Thus the presence of microscopic signs of ASR was considered as the indicator of ASR of the aggregates.

Chert-rich limestones were considered the most alkali-reactive aggregates in the investigated concrete samples. Their presence in three concrete samples increased the volume of alkali-silica gels up to 4.9 vol. %, and a large amount of cracks intruded into them. Thus, the volume of cracks could be quantified in these three samples.

Greywacke, meta-greywacke, meta-sediment, quartzite, and quartz aggregate represent the second group of alkali-silica reactive aggregates in concrete, present in eight concrete samples. From alkali-silica reactive aggregates of anthropogenic origin, slag was identified. The positive correlation of concrete ageing on increasing amounts of alkali-silica gels was observed.

Table 3. Comparison of macroscopic and microscopic signs of ASR in concrete samples. s.n. – sample number, ASG – alkali-silica gels, ASR c.a. – alkali-silica reactive coarse aggregates, ASR f.a. – alkali-silica reactive fine aggregates, f.f. – floor framing, q.a. – quartz aggregate.

| S. n. | Construction | Datation | Macroscopic damages (*) | Microscopic signs of ASR | ASG (vol. %) | ASR c.a. | ASR f.a. |
|---|---|---|---|---|---|---|---|
| 14-070 | Trutnov | 1977 | leaks into construction joints, deep concrete degradation, cracks in f.f. | ASG in pores (rarely) | 0.1 | - | - |
| 14-071 | Trutnov | 1975 | leaks in construction joints, cracks in f.f. | ASG in pores (rarely) | 0.1 | - | - |
| 180-010 | Dolany | 1934 | cracks in f.f., moulding surface, spandrel panel surface and in road-fence | ASG in pores and in contact with aggregates, ASR cracks, ASR boundaries | 0.7 | Quartzite, q.a., slag | - |
| 232-007 | Liblín | 1929 | cracks in f.f., in road surface and in spandrel panel surface | ASG in pores and in contact with aggregates, ASR cracks, ASR boundaries | 0.6 | Quartzite, q.a. | - |
| 272-006 | Lysá n. Labem | 1973 | out of drainage, in-leak, corrosion and ASR cracks in landing fronts | ASG in pores and in contact with aggregates, ASR cracks, ASR boundaries | 0.6 | Quartzite, q.a., metagreywacke | - |
| 610-018 | Stará Boleslav | 1982 | leaks into construction joints, corrosion and deep open cracks in f.f. surface | ASG in pores and in contact with aggregates, ASR cracks, ASR boundaries | 0.3 | Quartzite, metagreywacke | - |
| 610-019 | Tuřice | 1924 | cracks in f.f. surface, corrosion | ASG in pores and in contact with aggregates, ASR cracks | 0.7 | Quartzite, q.a. | - |
| 610-035 | Svijany | 1924 | leaks, corrosion, cracks in f.f. | ASG in pores and in contact with aggregates, ASR cracks, ASR boundaries | 0.8 | Quartzite, q.a., slag | - |
| Y531 | Malešice - Vršovice | 1996 | leaks into construction joints, cracks | ASG in pores (rarely) | 0.1 | - | - |
| X604 | Štěrbo-holy | 1990 | leaks into construction joints, cracks | ASG in pores and surrounding aggregate boundaries, ASR cracks | 0.6 | Q.a., metagreywacke , metasediment | - |
| MK7 | Choceň | 1955 | leaks into construction joints, corrosion, deep open cracks, cement paste leaching | ASG in pores and in contact with aggregates, ASR cracks | 0.9 | Quartzite, q.a. | |
| DB102 | Stadice | 1990 | leaks into construction joints, corrosion, deep open cracks, cement paste leaching | ASG in pores (rarely) | 0.1 | - | - |
| 2-3 | Mirotice | 1928 | leaks into construction joints, corrosion, deep open cracks, cement paste leaching | ASG in pores (rarely) | 0.1 | - | - |
| 1-2 | Mirotice | 1928 | leaks into construction joints, corrosion, deep open cracks, cement paste leaching | ASG in pores (rarely) | 0.1 | - | - |
| v6 | Prague | 2000 | leaks into construction joints, ASR cracks | ASG in pores and in contact with aggregates, ASR cracks, ASR boundaries | 4.9 | Chert-rich limestone | - |
| v9 | Prague | 2000 | leaks into construction joints, ASR cracks | ASG in pores and in contact with aggregates, ASR cracks, ASR boundaries | 2.3 | Chert-rich limestone | - |
| v11 | Prague | 2000 | leaks into construction joints, ASR cracks | ASG in pores and in contact with aggregates, ASR cracks, ASR boundaries | 3.1 | Chert-rich limestone | - |

# 3. Alkali-silica reaction - experimental testing of aggregates

## 3.1. Testing methods

"All aggregates are alkali-reactive; they differ only in the kind of reaction and the degree and rate" (B. Mather 1975 [94]). On the basis of Mather's hypothesis, there can be doubt about the purpose of aggregate testing. On the other hand, the testing of aggregates enables one to assess the limits, below which the ASR is safe for a concrete construction. The testing of aggregates eliminates those highly alkali-reactive aggregates and it can mitigate the alkali-silica reaction.

Three main groups of test methods are conventionally used: petrographic, dilatometric, and chemical. Petrographic methods are focused on the petrographic inspection of aggregates in the natural state. Aggregates are analysed using optical microscopy in thin sections, and classified according to their alkali-silica reactivity [55, 59, 95]. For example, the RILEM AAR-1 petrographic method [55] classifies aggregates into three groups: unlikely to be alkali reactive (*e.g.* granite, diorite), potentially alkali reactive (*e.g.* quartz aggregates, sediments and meta-sediments), and very likely to be alkali reactive (*e.g.* chert, opal, quartzite, glassy volcanic rock fragments). Aggregates tested using petrographic methods are classified with respect to their modal composition, and to the proportion of the three reactivity groups [55].

Chemical methods are applied on highly alkali-reactive aggregates. They classify aggregates according to the proportion of soluble $SiO_2$ and according to the decrease in alkalinity [57, 96]. Chemical methods are hardly applicable to slowly reactive aggregates, especially to quartz rich aggregates.

The dilatometric (mortar bar and concrete prism) methods are the most widely applied methods to determine alkali-silica reactivity potential of aggregates (*e.g.* [23, 52, 97 - 99]). The first subgroup, "normal" or "standard" mortar bar methods and concrete prism tests (*e.g.* [53, 100]), are based on the testing of large concrete prism specimens (40 × 40 × 160 mm), containing coarse aggregates as well as fine aggregates, in wet conditions above 40°C. Their disadvantage is regarded to be the long testing period (6 or 12 months). But some authors considered them to be the most realistic test for ASR [101]. The second subgroup is presented by accelerated mortar bar methods (ASTM C227 [102], ASTM C1260 [53], NP1381 [103], P 18-588 [104]), based on the testing of thin mortar bar specimens (25 × 25 × 285 mm) in alkaline solutions at 80°C, both accelerating the ASR. All aggregates tested, using mortar bar methods, are required

to be crushed into the size fraction 0/4(5). The mortar bar methods are applicable on all rock types. For example, using the accelerated mortar bar method ASTM C1260, the aggregates are classified according to the expansion of mortar bar specimens after a 14 day test period for accelerated tests (*viz.* after 6 moths testing period for "standard" tests). Aggregates are classified according to the expansion ($\Delta$) values as [53]: I. Reactive - $\Delta > 0.200$ %, II. Potentially reactive - $\Delta = 0.100 - 0.200$ %, III. Non reactive $\Delta < 0.100$ %.

A special type of petrographic method, although rarely used, is the gel pat test. Its principle is based on the macroscopic investigation of aggregates incorporated in the mortar pat specimens, with the aim to identify opal-rich aggregates. The method combines two main advantages: aggregates are examined macroscopically and their ASR potential is determined directly, according to the origin of alkali-silica gels. The disadvantages of the original gel pat test are regarded as the lack of quantification of ASR potential (comparable with expansion of mortar bar specimens) and the limitation of the test conditions to extremely reactive aggregates.

Three test methods were chosen for experiments in this study:

I. The RILEM AAR-1 petrographic method, with the objective to verify the possible application of petrographic methods on testing of quartz-rich aggregates from the Czech Republic.

II. The ASTM C1260 accelerated mortar bar method - with the objective to classify the ASR potential of samples, using one of the most frequently used methods. Thus, the ASR potential of the studied samples is possible to be compared with the aggregates tested in practice.

III. The gel pat test - however, originally designed for testing of different aggregates, the method was chosen, due to the possible combination for examination of aggregates with their testing in a mortar environment.

## 3.2. Aggregates

Aggregates tested for their alkali-silica reactivity potential were sampled from 20 sand pits representing Quaternary sands and gravels from areas around the Cidlina, Dyje, Labe, Ohře and Sázava rivers (Czech Republic). The samples (see Table 4) were processed by sieve separation of grain size fraction > 4 mm, and macroscopic description. Fraction 0/4 was used for the experiments.

Table 4. Samples of quartz sands and gravels.

| Sample no. | Location | Fraction (mm, in weight %) | | | | |
|---|---|---|---|---|---|---|
| | | > 4 | 2/4 | 0.1/2 | < 0.1 | Total |
| 56 | Vrbová Lhota | 9.5 | 15.9 | 73.3 | 1.3 | 100 |
| 69 | Dřenice | 62.9 | 14.7 | 20.8 | 1.5 | 100 |
| 79 | Toušeň | 7.6 | 7.3 | 83.5 | 1.5 | 100 |
| 179 | Hradišťko I. | 37.3 | 4.0 | 57.8 | 0.9 | 100 |
| 181 | Staré Ždánice | 15.6 | 7.8 | 76.1 | 0.5 | 100 |
| 208 | Roudnice ACHP | 40.5 | 9.2 | 48.4 | 2.0 | 100 |
| 211 | Beleč Marokánka | 21.8 | 11.3 | 66.2 | 0.6 | 100 |
| 279 | Velký Luh | 38.5 | 29.9 | 27.2 | 4.4 | 100 |
| 280 | Soběsuky | 59.3 | 8.9 | 29.7 | 2.1 | 100 |
| 350 | Pamětník | 53.9 | 8.9 | 35.2 | 2.0 | 100 |
| 372 | Hlavačov | 46.4 | 14.5 | 35.9 | 3.2 | 100 |
| 653 | Roudnice Sušárna | 24.3 | 13.5 | 61.3 | 0.8 | 100 |
| 668 | Bratřice | 2.6 | 13.1 | 82.4 | 1.9 | 100 |
| 676 | Tasovice | 7.2 | 12.5 | 75.4 | 4.9 | 100 |
| 1024 | Provodín Jižní II | 7.0 | 3.8 | 86.5 | 2.7 | 100 |
| 1025 | Čeperka Oplatil | 7.0 | 15.0 | 76.0 | 2.0 | 100 |
| 1027 | Kaznějov | 7.8 | 13.3 | 77.8 | 1.1 | 100 |
| 1032 | Obruby | 27.9 | 14.7 | 56.5 | 0.8 | 100 |
| 1033 | Čermuc | 20.1 | 14.1 | 65.3 | 0.5 | 100 |
| 1279 | Kluk | 16.5 | 9.6 | 69.6 | 4.3 | 100 |

## 3.3. Modified petrographic RILEM AAR-1 method

### 3.3.1. The RILEM AAR methods

RILEM AAR [105] is a group of methods applied-for the ASR testing of aggregates. The RILEM test methods are based on British National Standards. Their re-writing and re-development was initiated, due to the lack of national standards that applied to aggregate testing validated in other countries. In the future, the modified RILEM methods should be applicable in other countries as European or International standards [105, 106].

The RILEM AAR-1 petrographic method [55] represents a method used to determine the ASR potential of aggregates, based on their petrographic classification. Its use for determination of

the ASR potential of aggregates was performed with the objective to verify its potential usability in the Czech Republic. In the case of successful application, the method should be incorporated in the Czech National Standards or technical guides (*e.g.* in [60]).

### 3.3.2. Modification of RILEM AAR-1 method by petrographic image analysis

The classification of the ASR potential of aggregates, using the RILEM AAR-1 petrographic method, is based on the classification of individual rock and mineral types into the three following groups: very likely to be alkali reactive, potentially alkali reactive, and unlikely to be alkali reactive. Rocks and minerals are classified using the conventionally-accepted experience about their reactivity (*e.g.* granitoids are accepted as unlikely to be alkali reactive, quartz and quartz rich rocks are potentially reactive, and volcanic glass is very likely to be alkali reactive). A complete list of rocks and minerals and their ASR classification is mentioned in Annex A.1.2. - A.1.3. in the RILEM AAR-1 method [55].

The detailed application of the RILEM AAR-1 method on investigated quartz sands and gravels is discussed in Appendix B. Its comparison with other test methods applied on aggregates testing is included in Appendices C and D. The system of quantification of individual rock and mineral types in thin sections is based on the point counting of thin sections in an optical microscope. Its accuracy is limited by the number of counts per thin section. The RILEM AAR-0 method requires 500 counts per thin section [55].

Modern methods, such as petrographic image analysis, allow more accurate determinations of the modal composition of thin sections. The points in thin sections are counted automatically using computer software, and their density is higher than original point counting in an optical microscope. The use of the computer-assisted method is accompanied by a decrease in time per thin-section (*e.g.* [84]). The petrographic image analysis can be used in concrete investigation, as well as in the classification of natural rock. Other important advantages of petrographic image analysis are regarded as the possible determination or the geometric characteristics of aggregates, such as perimeter and length of minor or major axis. The main advantage of petrographic image analysis, in respect to the ASR potential of aggregates is regarded to be the more accurate determination of the modal composition of concrete samples, determination of petrographic composition and structural parameters of aggregates, and the determination of the volume of alkali-silica gels.

The results obtained using both methods, point counting and petrographic image analysis, were compared. For a more detailed view, see Appendix B. The comparison pointed-out the most important disadvantage of the RILEM AAR-1 petrographic method [55] is the unappreciated quantification of the volume of individual phases, which affects the accuracy of the entire method. The point counting systematically underestimates the volume of particles showing an irregular shape, *e.g.* elongated and/or curved particles. In contrast, volumes or circular particles are overestimated (see Appendix B).

The systematic comparison of ASR classification of aggregates, following the RILEM AAR-1 petrographic method (although modified by petrographic image analysis, with classification of aggregates following dilatational methods) pointed-out other disadvantages (see Appendix E). The classification of aggregates according to the RILEM AAR-1 petrographic methods is poorly correlated with expansion values. The main reasons could be:

- Insufficiently classified petrographic examination of aggregates caused by a low-level of experience of the petrographer with such microscopic investigation.
- Insufficient determination of the petrographic characteristics of aggregates, causing an incorrect classification of the aggregates.
- The classification of aggregates by the RILEM AAR-1 method is based on the general assumption about their ASR potential. However, the same rock types can differ in their mineralogical composition, degree of deformation, and origin. Thus their differential ASR potential is possible. The ASR potential of aggregates is impossible to measure in real cement conditions, and aggregates are not evaluated according to their behaviour in cement or concrete.

## 3.4. Accelerated mortar bar ASTM C1260 method

### 3.4.1. Accelerated mortar bar methods

The mortar bar tests (*e.g.* [53]) represent the most frequently used approach to assess the ASR potential of aggregates (*e.g.* [23, 25, 97 - 99]), as well as to evaluate the effect of mineral admixtures mitigating the ASR [107, 108]. The accelerated tests are based on the measurement of expansion values reflecting the amounts of alkali-silica gels originating, due to the significant content of alkali reactive aggregates (*e.g.* [98, 99]).

Mortar bar tests can be divided into two subgroups: "normal" and accelerated mortar bar tests, differing mainly in the length of the testing period, size of mortar specimens, and the use of alkaline solution (respectively, chambers maintaining wet conditions, *e.g.* [33, 99]). The mortar bar methods are preferentially used due to their possible application on the testing of all aggregates, without respect to their origin or composition. The time factor also plays an important role (*e.g.* [98, 99]).

### 3.4.2. Investigation of ASR potential of quartz sands and gravels according to expansion values of mortar bar specimens

Although, "standard" mortar bar tests [56, 100] could be applied on slowly reactive aggregates, they tend to underestimate the ASR potential of aggregates (*e.g.* [2, 33, 52]). Accelerated mortar bar tests are regarded to be more successful, due to the application of alkaline solutions and high temperature. Thus, the accelerated mortar bar test ASTM C1260 was applied on the studied quartz sands and gravels. The experimental work aimed to: quantify their ASR potential; obtain suitable mortar specimens usable in future microscopic investigations; and to verify the accuracy of the sampling, based on the comparison of the expansion values of aggregates from the same deposits but sampled at different times. The application of the accelerated mortar bar method ASTM C1260 on quartz sands and gravels is discussed in Appendix C.

### 3.4.3. Modification of ASTM C1260 method by petrographic image analysis of thin sections

Petrographic methods (*e.g.* optical and electron microscopy) are fundamental methods in the investigation of signs of ASR in concrete (*e.g.* [29, 31, 45, 47, 109]). They enable direct identification of alkali-reactive aggregates and contribute to the understanding of ASR mechanisms (Appendix C).

In this study, the petrographic methods were applied on thin-sections prepared from mortar bar specimens containing the studied quartz sands and gravels, after the ASTM C1260 test, with the objective to observe the amount of alkali-silica gels and the locations of their formation. The same approach, including computer-assisted image analysis (as described for the quantitative study of original sands according to modified RILEM AAR-1 method) was applied.

The optical microscopy and petrographic image analysis enables one to identify alkali reactive components of sands and gravels, according to their spatial relationship with the ASR products. Thus, ASR was caused mostly by volcanic, quartzite, and quartz fragments. In contrast no evidence of ASR was observed in connection with granitoids, feldspar, and mica fragments (see Appendix C).

The quantitative assessment of individual phases in mortar bar samples was compared with the expansion values of mortar bar specimens (see Appendix C). The highest correlation factor was calculated for the correlation of the expansion values with the volume of alkali-silica gels (see Fig. 3, part a, in Appendix C). This confirms the fact that the expansion is caused by the origin of alkali-silica gels in the mortar bar specimens.

### 3.4.4. Impact on sampling methodology

The same quartz sands and gravels, taken from the same deposits, were tested as a part of another project three years ago [52]. The samples were investigated using chemical methods (following the ČSN 72 1178 and ČSN 72 1179 standards [56, 57]) and using mortar bar methods (following the ČSN 72 1179 standard and the ASTM C1260 standard [53]).

The application of the same testing methods (performed in the same testing laboratory) to the testing of the same aggregates enabled us to compare conditions of sampling and splitting. Thus, the results obtained from the dilatational testing (following ASTM C1260 standard [53]) performed in 2001 were compared with those from 2006.

Surprisingly, differences were found in all 20 samples. The difference exceeded a difference of more than 50% of the initial value, in the case of four studied samples (Tab. 5). The change of expansion values caused a different classification of the ASR potential in another five cases (pointed-out by the grey colour of cells in Tab. 5). This points-out the importance of a revision of standards used in the sampling of sedimentary deposits in the Czech Republic. The heterogeneity of sedimentary deposits is well known, and difficulties with their representative sampling and testing have caused decreasing interest in their exploration [52].

Table 5. Comparison of expansion values (Δ) of mortar bar specimens containing studied samples. Δ (%) 2001 - expansion value measured in 2001, Δ (%) 2006 - expansion value measured in 2006, DIV - absolute value of difference from initial value (in %), SMD - standard mean deviation. Grey colour of the cells - different classification of ASR potential of the samples according to [53].

| Sample no. | 56 | 69 | 79 | 179 | 181 | 208 | 211 | 279 | 280 | 350 |
|---|---|---|---|---|---|---|---|---|---|---|
| Δ (%) 2001 | 0.174 | 0.047 | 0.165 | 0.167 | 0.225 | 0.158 | 0.117 | 0.090 | 0.054 | 0.134 |
| Δ (%) 2006 | 0.180 | 0.049 | 0.140 | 0.132 | 0.211 | 0.194 | 0.133 | 0.041 | 0.091 | 0.137 |
| DIV (%) | 3.4 | 4.3 | 15.2 | 21.0 | 6.2 | 22.8 | 13.7 | 54.4 | 68.5 | 2.2 |
| SMD | 0.0025 | 0.0000 | 0.0020 | 0.0000 | 0.0010 | 0.0015 | 0.0005 | 0.0005 | 0.0015 | 0.0010 |
| Sample no. | 372 | 653 | 668 | 676 | 1024 | 1025 | 1027 | 1032 | 1133 | 1279 |
| Δ (%) 2001 | 0.103 | 0.165 | 0.048 | 0.084 | 0.067 | 0.212 | 0.280 | 0.109 | 0.115 | 0.224 |
| Δ 2006 | 0.086 | 0.189 | 0.024 | 0.028 | 0.044 | 0.188 | 0.217 | 0.086 | 0.087 | 0.122 |
| DIV (%) | 16.5 | 14.5 | 50.0 | 66.7 | 34.3 | 11.3 | 22.5 | 21.1 | 24.3 | 45.5 |
| SMD | 0.0000 | 0.0030 | 0.0000 | 0.0000 | 0.0000 | 0.4980 | 0.0030 | 0.0015 | 0.0000 | 0.0000 |

## 3.5. Modified gel pat test combined with petrographic examination of alkali reactive aggregates in gel pat specimens

### 3.5.1 Gel pat test

The gel pat test was originally designed for quick identification of opal-rich aggregates [110]. The principle of the method is based upon the identification of opal-rich particles according to their ASR in the mortar pat samples. The ASR should be shown by macroscopically visible alkali-silica gels forming on the surface of the pat specimens. Although it represents a feasible method, requiring a minimum of laboratory equipment and sample preparation, it is rarely used (*e.g.* [111]).

The experimental conditions of this method are regarded to be unsatisfactory for most types of aggregates. The expected time period of testing is also too short for slowly reactive aggregates, such as quartz-rich rocks. The greatest drawback of the entire method was pointed-out by Fournier [111], who drew attention to the absence of quantification of the ASR potential of aggregates in the gel pat method. Also, the method does not need to be limited to the macroscopic identification of opal rich aggregates, but can applied on the general identification of aggregates reactive in mortar conditions.

### 3.5.2 Investigation of ASR potential of quartz sands and gravels according to the modified gel pat test

The two main advantages of the gel pat test, petrographic examination of aggregates and investigation of their ASR potential in mortar conditions, seemed to be useful to test the ASR potential of quartz sands and gravels. The main requirements for this application were to modify test conditions, with respect to slowly reactive aggregates, as well as to develop a method to exactly determine the ASR potential of aggregates in gel pat specimens (see Appendix D).

Our major improvement of the gel pat test methodology (with the exception of the changes in solution composition and in the time period) has been regarded as the application of optical microscopy and petrographic image analysis for the quantification of the ASR potential of aggregates, based on the determination of the volume of alkali-silica gels in the gel pat specimens. Alkali-silica gels (as well as ASR cracks) are identified in three different steps: on the macroscale using a magnifying glass, on the microscale using an optical microscope, and using SED/EDS analysis to evaluate their chemical composition and morphology (see Appendix E). The ASR potential of quartz sands and gravels (determined by using a modified gel pat test), was correlated with the ASR potential of aggregates; determined by using a modified mortar bar method (for more detailed information see Section 3.7 and Appendix D). Satisfactory correlation factors were obtained from the relationship of the expansion values with the number of alkali-reactive fragments, and the volume of alkali-silica gels in the gel pat specimens.

## 3.6. ASR of quartz-rich aggregates – influence of deformation and recrystallization characteristics

### 3.6.1. ASR of quartz-rich aggregates - an unsolved problem

Quartz-rich aggregates (a widely discussed topic since the 2$^{nd}$ half of the 20$^{th}$ century) are used as a general term to denote rocks of different origins, basically composed of quartz (*e.g.* quartzite, quartz gneiss, phyllite, schist, quartz sandstone, and siltstone). The specific term "quartz aggregate" is used to mark aggregates with a quartz content higher than 95 vol. %, whose classification can not be specified (*e.g.* segregation quartz, vein quartz) without some knowledge about the source location [112, 113]. The ASR of quartz-rich aggregates is an unsolved problem, whose importance resides in the extensive use of quartz-rich aggregates in civil engineering (*e.g.* [2, 9, 18, 19, 23, 26, 98]).

The ASR of quartz-rich aggregates was investigated from the following points of view:

- Quartz undulatory extinction.
- Grain size.
- Deformation and recrystallization characteristics.
- Effect of minor elements contained within the quartz.
- Effect of secondary minerals contained in the aggregates.

The undulatory extinction of quartz is the result of several low-angle boundaries, separating areas with different crystal orientations. Well-crystallized quartz, containing minimal amounts of areas with undulatory extinction and subgrains, is non-reactive (or very minimally reactive) in ASR. By contrast, strongly deformed and alkali reactive quartz contains large areas with subgrains and undulatory extinction [114].

Previously, the ASR potential of quartz-rich aggregates was estimated by the angle of undulatory extinction [18, 115-117]. Those aggregates with an angle of undulatory extinction higher than 15° were accepted as potentially reactive. Several authors [115, 116, 117] published their reservations about the usability of the angle of undulatory extinction, and its correlation with the ASR potential of aggregates. They pointed-out that the influence of deformation characteristics and the presence of microcrystalline quartz are the most important factors in the ASR of aggregates. These conclusions were also confirmed by French [36] and Zhang *et al.* [20]. In this recent research, the ASR potential of quartz is compared with grain size and the specific surface area of aggregates [26, 95, 118, 119]. Their successful application has not yet been confirmed in a large number of aggregates.

### 3.6.2. Alkali reactive quartz-rich aggregates in sands and gravels and recrystallization mechanisms

ASR (AAR) of aggregates in concrete is a complex problem, reflecting the factors of aggregate composition, alkalis content in cement (and its solution from aggregates), and moisture content [7, 22]; and impossible to be investigated separately from the other parameters. Increasing content of alkalis in cement, as a result of alkalis leaching from aggregates, causes increasing degrees of ASR in concrete. Finally, aggregates accepted as non-reactive could react [119]. In recent research, there is a lack of intricate descriptions of the parameters needing to be investigated in connection with the ASR of quartz-rich aggregates.

As a part of this PhD study, a system for classifying the deformation and recrystallization mechanisms in quartz aggregates was chosen [120], with the objective to find a more appropriate correlation of the expansion of the mortar bar specimens to the results of petrographic investigations [82]. The angle of undulatory extinction was not determined, due to its frequent criticism in the literature (*e.g.* [2, 9, 18, 19, 23, 26]). The classification system chosen was originally formulated by Stipp *et al.* [120], interconnecting the degree of quartz recrystallization with the grain size characteristic and temperature (based on the conclusions in [121 - 123]). The sensitivity of the whole classification to grain-size parameters proposed a preferential use in sand and gravel investigations [82].

Dynamic recrystallization (recrystallization simultaneous to deformation), defined by Stipp *et al.* [120] is divided into three main stages: bulging (BLG), subgrain rotation (SGR), and grain boundary migration (GBM). The BLG mechanism is active at temperatures of 280 - 400°C (at pressures of 2.5 - 3.0 kb), characterised by bulging or embayment boundaries, containing newly-formed grains of a few μm in diameter (Fig. 7). With increasing temperature, the BLG mechanism transforms to the SGR mechanism (temperatures of 400 - 500°C), characterised by increasing size of newly formed grains (60 - 100 μm in diameter), generating a mosaic texture (Fig. 8). Constantly increasing temperature (over 500°C) causes transformation of the SGR mechanism into the GBM mechanism. Newly formed grains exceed 120 μm in diameter [120].

During the initial stage, three mortar bar specimens, prepared from three samples of sands and gravels were selected for more detailed study. Thin sections, prepared from each specimen, were analyzed using petrographic image analyses. Their modal composition was calculated with the objective to determine the content of quartz aggregates recrystallized in individual recrystallization mechanisms, in order to determine their relationship with alkali-silica gels and to calculate the volume of alkali-silica gels (Tab. 6).

A positive association was found between the expansion of the mortar bar specimens and the volume of quartz-rich aggregates recrystallized in both the BLG mechanism, SGR mechanism, and their transitions. A positive association was also found between these recrystallization regimes and the volume of the alkali-silica gels in the mortar bar specimens. No correlation was found between the volume of quartz-rich aggregates recrystallized in the GBM regime and the expansion of mortar bar specimens, as well as the volume of alkali-silica gels (Fig. 9).

Table 6. Modal composition of thin-sections prepared from three different mortar bar specimens. Recognised recrystallization mechanisms are following: bulging (BLG), subgrain rotation (SGR), grain boundary migration (GBM) and their combination (BLG-SGR, BLG-GBM). Data in vol. %. Mortar bar specimens containing samples of sands and gravels no. 181, 208, and 280 (locations Staré Ždánice, Roudnice ACHP, and Soběsuky).

| Mortar bar specimen no. | 181a | 208b | 280a |
|---|---|---|---|
| Cement paste | 50.37 | 56.30 | 29.70 |
| Pores | 5.20 | 2.60 | 1.10 |
| Alkali-silica gels | 5.90 | 6.10 | 0.01 |
| Fragments without any relationship to ASR | 30.22 | 25.91 | 68.48 |
| Fragments recrystallized in BLG mechanism | 2.75 | 2.53 | - |
| Fragments recrystallized in SGR mechanism | 5.45 | 4.76 | 0.30 |
| Fragments recrystallized in GBM mechanism | 0.11 | 0.38 | 0.23 |
| Fragments recrystallized in BLG-GBM mechanism | - | 1.42 | - |
| Fragments recrystallized in BLG-SGR mechanism | - | - | 0.19 |
| Total | 100.00 | 100.00 | 100.00 |

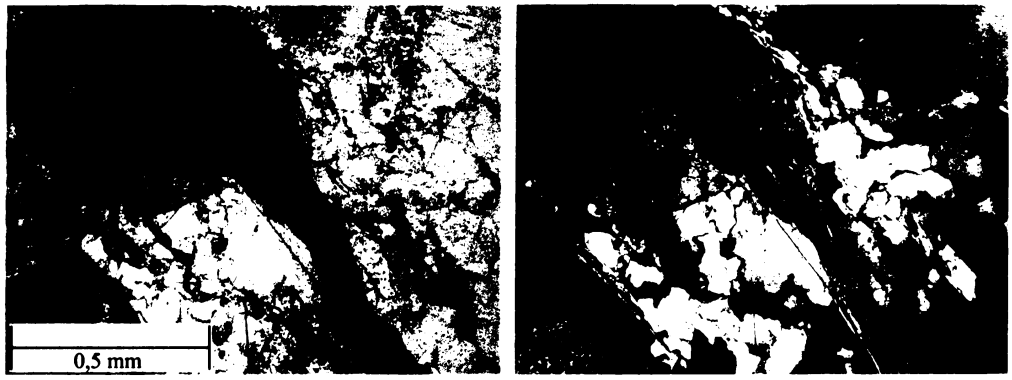


Figure 7. Two quartz-rich aggregates recrystallized by BLG mechanism. Alkali-silica gel is situated in left upper edge of micrographs. Optical microscope, parallel (on the left) and crossed (on the right) nicols. Thin section no. 208b prepared from mortar bar specimen. Mortar bar specimen containing sample no. 208 from the Roudnice deposit ACHP.

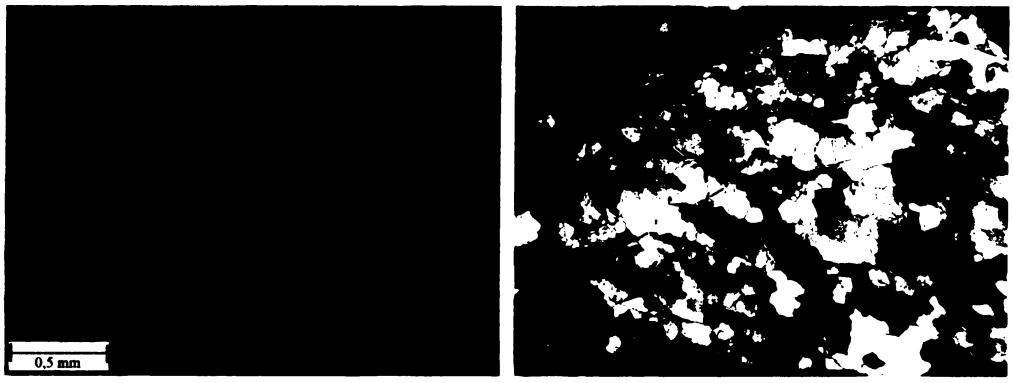


Figure 8. Quartz-rich aggregate recrystallized by the SGR mechanism. Optical microscope, parallel (on the left) and crossed (on the right) nicols. Mortar bar specimen containing sample no. 181 from the Staré Ždánice deposit.

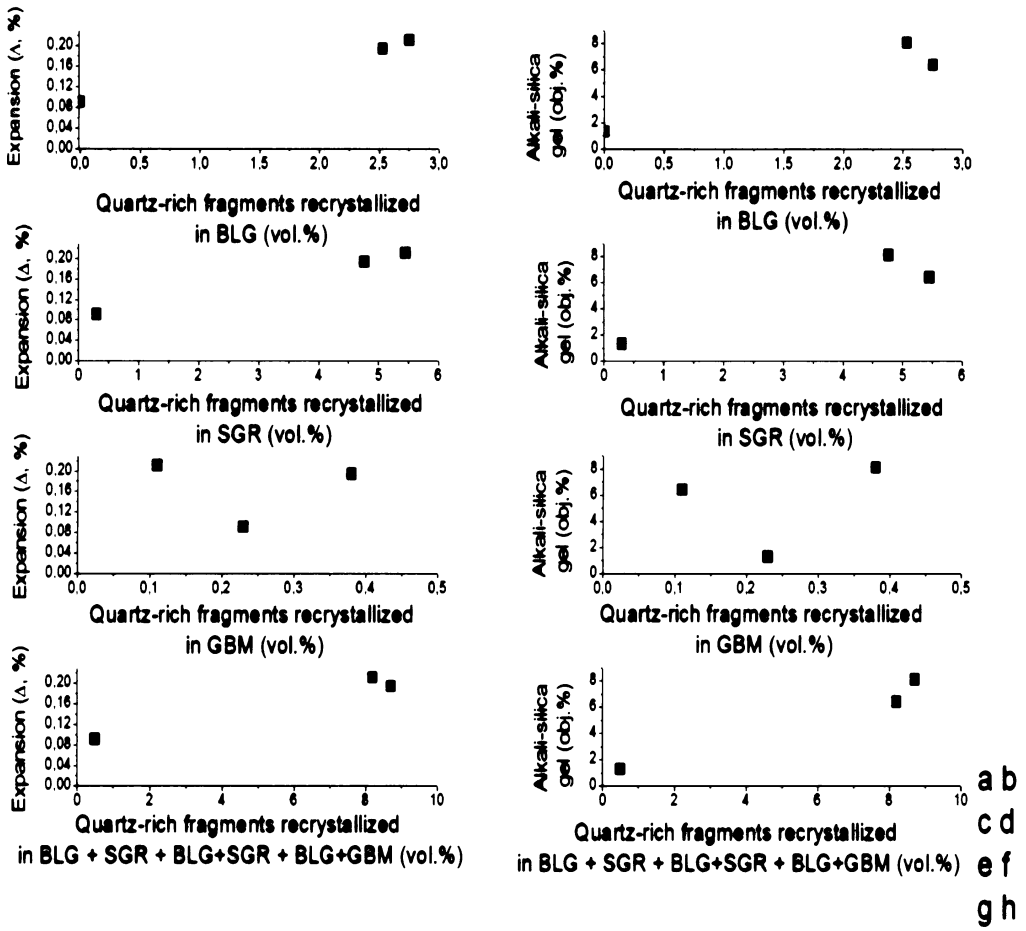


Figure 9. Comparison of expansion (*viz.* volume of alkali-silica gels in mortar bar specimens) and volume of quartz-rich fragments recrystallized by the BLG mechanism (a, b), SGR mechanism (c, d), GBM mechanism (e, f), BLG + SGR + BLG/SGR + BLG/GBM mechanisms (g, h).

### 3.6.3. Summary - recrystallization in quartz sands and gravels

A detailed petrographic investigation of quartz recrystallization in the studied sands and gravels elucidated:

- Quartzite fragments (identified in petrographic investigation of mortar bar specimens) are more appropriately classified as quartz aggregates (containing a minor volume of other minerals).
- Using optical microscopy and petrographic image analysis, the recrystallization mechanisms can be investigated in mortar bar specimens. This approach enables one to relate the signs of ASR to define the ASR potential of aggregates, and to classify the aggregates with regard to their mineralogical composition and recrystallization characteristics.
- The BLG and SGR recrystallization mechanism seems to be responsible for the ASR of quartz aggregates. In contrast, the GBM mechanism exhibits no relationship with ASR.
- A possible explanation is primarily to be found in the grain size parameters of newly formed quartz grains, from the individual deformation mechanism. Quartz fragments recrystallized by the BLG mechanism (characterised by newly formed quartz grains of a few μm in diameter) are more responsible for ASR, than coarse-grained aggregates recrystallized by the GBM mechanism.

A similar association between the recrystallization mechanism and the ASR potential of quartz-rich aggregates, as discussed above, was also observed in aggregates in concrete samples. A more detailed investigation of quartz aggregates in concrete samples, including quantitative points of view, is needed for future research. Larger numbers of studied samples (mortar bar specimens as well as concrete samples) can increase the accuracy and credibility of the investigation.

## 3.7. Discussion and summary on aggregates testing and classification of their ASR potential

In practice, the petrographic, mechanical, physical, and chemical properties of aggregates (including their ASR potential) affect their usability. The maximum requirements are imposed on aggregates used in concrete constructions subjected to high precipitation or sea water spray. Requirements are directly proportional to the degree of the expected mechanical loading of the construction; *e.g.* higher requirements are imposed on aggregates used in airport runways and

motor highways, than on aggregates used for local roads. In the case of indoor constructions, not exposed to precipitation and surface humidity, the use of aggregates is not so restricted (*e.g.* [2, 36, 88, 124 - 126]).

The sands and gravels investigated are used commercially in concrete prepared for outdoor constructions, especially in concrete pavement of highways. Thus, the aggregates must fulfil the requirements connected with their low ASR potential. As the final stage of sand and gravel testing, it was essential to formulate a classification of aggregates, with respect to ASR. Three main methods (modified RILEM AAR-1 method, mortar bar ASTM C1260 method, and gel pat test) classify the aggregates; differing from each other, based on the petrographic and expansion characteristics. Aggregates classified as reactive are not suitable for outdoor concrete constructions.

A simple classification (RILEM AAR-1 [55]) of aggregates, according to their generally accepted reactivity, distinguishes rocks that are: (1) unlikely to be alkali-reactive (holocrystalline plutonic igneous rocks such as granites, non-reactive minerals - feldspars, micas, pyroxene); (2) potentially alkali-reactive (quartz, sedimentary rock such as quartz-rich aleurites, sandstones and siltstones, or some metamorphic rocks, such as phyllites); and (3) very likely to be alkali-reactive (quartzite, silicite or glass-bearing volcanic rocks). It does not specify the classification of aggregates containing more than one phase, with different ASR potentials. Sandstone and siltstones are classified as potentially reactive with respect to the quartz content. Quartz sands and gravels are not directly named. Thus, it was necessary to combine the classification of individual phases contained in the sands and gravels, and to assign new limits applicable on the studied samples. The classification of the samples mainly containing quartz fragments must be accepted, with the following note: their potential alkali-reactivity was assigned using conventional mineralogical classification, and no deformation structures or angles of undulatory extinction were investigated.

The number of phases very likely to be alkali-reactive (*viz.* potentially alkali-reactive and unlikely to be alkali-reactive), exceeding 50 % of the total volume of the aggregates, was accepted as a critical parameter. Samples containing more than 50% of phases very likely to be alkali-reactive (*viz.* potentially alkali-reactive and unlikely to be alkali-reactive) are classified as very likely to be alkali-reactive (*viz.* potentially alkali-reactive and unlikely to be alkali-reactive) samples (see Tab. 7).

Dividing the aggregates into three groups, according their ASR potential, is also characteristic for the ASTM C1260 mortar bar method. Aggregates classified as alkali reactive exhibit the

expansion value $\Delta > 0.200\%$ (*viz.* $\Delta = 0.200 - 0.100$ for potentially reactive aggregates, and $\Delta < 0.100$ for non reactive aggregates. The expansion, measured according to the ASTM C1260 [53] method and the classification is shown in Tab. 8.

Table 7. Classification of ASR potential of the studied samples, according to the modified RILEM AAR-1. Total - ARP (*viz.* PARP, NARP) - total amount of phases very likely to be alkali-reactive (*viz.* potentially alkali-reactive phases, unlikely to be alkali-reactive phases). (*) - classification was impossible, according to the volume of phases exceeding 50 % of total, but it was selected according to the prevailing types of phases. (**) - volume of three types of phases is comparable.

| Sample no. | Total-ARP | Total-PARP | Total-NARP | Classification (RILEM AAR-1) |
|---|---|---|---|---|
| 56 | 39.6 | 48.8 | 11.6 | PARP (*) |
| 69 | 4.0 | 94.8 | 0.0 | PARP |
| 79 | 15.6 | 79.9 | 4.5 | PARP |
| 179 | 8.0 | 79.3 | 12.7 | PARP |
| 181 | 25.2 | 66.1 | 7.7 | PARP |
| 208 | 26.4 | 58.4 | 15.2 | PARP |
| 211 | 8.9 | 67.4 | 23.7 | PARP |
| 279 | 23.4 | 76.5 | 0.0 | PARP |
| 280 | 43.8 | 43.8 | 12.0 | ARP-PARP (*) |
| 350 | 52.8 | 33.9 | 13.4 | ARP |
| 372 | 25.6 | 74.4 | 0.0 | PARP |
| 653 | 34.4 | 33.8 | 31.3 | ARP-PARP-NARP(**) |
| 668 | 3.1 | 23.3 | 72.1 | NARP |
| 676 | 6.5 | 60.6 | 32.9 | PARP |
| 1024 | 13.5 | 86.4 | 0.0 | PARP |
| 1025 | 52.8 | 38.7 | 8.5 | ARP |
| 1027 | 28.2 | 70.4 | 1.0 | PARP |
| 1032 | 19.7 | 69.5 | 10.8 | PARP |
| 1033 | 12.6 | 49.6 | 36.1 | PARP-NARP (*) |
| 1279 | 20.1 | 75.8 | 4.1 | PARP |

Using both methods, only one sample, unlikely to be alkali-reactive (according to RILEM AAR-1), and six potentially alkali-reactive samples showed the same ASR rating. The ASR rating of the other thirteen samples is different, depending on the method used. Most of the changes occurred in samples classified as potentially alkali-reactive (according to the RILEM AAR-1 method). The ASTM C1260 test classified them as non-reactive. Other changes occurred between potentially alkali-reactive samples (according to the RILEM AAR-1 method),

reclassified as reactive samples (according to the ASTM C1260 method); and with very likely to be alkali-reactive samples (according to the RILEM AAR-1 method), reclassified as potentially reactive (according to the ASTM C1260 method).

Table 8. Classification of ASR potential of studied samples according to ASTM C1260 method, volume of alkali-silica gels in mortar bar specimens and in gel pat specimens, and according to the number of alkali reactive particles in gel pat specimens. R (*viz.* PR, NR) - reactive sample (*viz.* potentially reactive sample, non-reactive sample, classification according to the ASTM C1260 method). ASG - alkali-silica gels, s. - specimens, n.a. - not analyzed.

| Sample no. | Expansion (Δ, %) | Classification (ASTM C1260) | ASG in mortar bar s.(vol.%) | % of ASR particles in gel pat s. | ASG in gel pat s. (vol. %, GP) |
|---|---|---|---|---|---|
| 56 | 0.18 | PR | 5.9 | na | na |
| 69 | 0.049 | NR | 0.1 | na | na |
| 79 | 0.14 | PR | 1.8 | na | na |
| 179 | 0.132 | PR | 3.7 | 5.5 | 0.5 |
| 181 | 0.211 | R | 6.4 | 16.9 | 1.2 |
| 208 | 0.194 | PR | 8.1 | 18.3 | 2.1 |
| 211 | 0.133 | PR | 2.9 | na | na |
| 279 | 0.041 | NR | 0.0 | 0.0 | 0.0 |
| 280 | 0.091 | NR | 1.3 | na | na |
| 350 | 0.137 | PR | 3.6 | 5.6 | 0.8 |
| 372 | 0.086 | NR | 3.2 | na | na |
| 653 | 0.189 | PR | 5.2 | 4.7 | 1.0 |
| 668 | 0.024 | NR | 0.2 | 0.0 | 0.0 |
| 676 | 0.028 | NR | 0.0 | 0.0 | 0.0 |
| 1024 | 0.044 | NR | 0.0 | 0.0 | 0.0 |
| 1025 | 0.188 | PR | 5.1 | na | na |
| 1027 | 0.217 | R | 9.4 | 14.1 | 1.9 |
| 1032 | 0.086 | NR | 0.3 | na | na |
| 1033 | 0.087 | NR | 1.0 | na | na |
| 1279 | 0.122 | PR | 4.0 | na | na |

Classification of sands and gravels, according to the gel pat test, is scarcely definable, due to its original specification to opal-rich aggregates and due to the large improvements realized as a result of this study. The same reasons disqualify the classification of studied samples according to the petrographic analysis of mortar bar and gel pat specimens. Classifications according to these three methods are listed in Tab. 8, as the number of alkali reactive aggregates (determined according to modified gel pat test) and as the volume of alkali-silica gels (determined using

petrographic image analysis of mortar bar and gel pat specimens). In the next step, the expansion value was concluded as referential, and other methods were compared with it.

A stronger association was found in the comparison of expansion values with the volume of alkali-silica gels in mortar bar and gel pat specimens (*viz.* with number of alkali reactive particles in gel pat specimens), than in the comparison of expansion values with the classification of aggregates (according to the modified RILEM AAR-1 petrographic method). Expansion values are positively associated with the volume of alkali-silica gels in mortar bar specimens. This conclusion confirms the conventionally accepted fact that the expansion is mainly caused by ASR (see Fig. 4 in Appendix C).

Low correlation factors were calculated in comparison to the expansion values, with the total amounts of individual rocks (and minerals) identified in mortar bar specimens, as well as in gel pat specimens (see Appendix C and D). It indicates the lack of more detailed petrographic investigations of aggregates, including structural and textural parameters, grain size and the appropriate quantification of modal composition of rock fragments; pointed-out recently by several authors (*e.g.* [18, 118]).

A correlation was found between the expansion values and the results of the modified gel pat test. Both the number of alkali-reactive particles and the volume of alkali-silica gels in the gel pat specimens correlated positively with the expansion values of the mortar bar specimens (see Fig. 5 in Appendix E).

# 4. ASR products: their chemistry and morphology

## 4.1. Introduction to ASR products

The alkali-silica gels, the main products of ASR, are hydrated amorphous compounds of $SiO_4^{(4-)}$, alkalis, and minor elements in variable proportions. In thin-sections, alkali-silica gels are colourless, usually conchoidally cracked (due to drying of the gel during sample preparation). They exhibit a mean refractive index of 1.48 - 1.49, with an upper limit of 1.51 and a lower limit of 1.45 [127]. Their ability to absorb large amounts of water leads to considerable changes in volume (expansion). Expansion, characterised by expansive pressure (generally not exceeding 6 to 7 MPa [128]), creates tensile strain within the concrete, and causes cracking. It is influenced by the total amount of alkali-silica gel and its composition [2], but the quantitative relationship has not yet been determined.

The macroscopically-visible extent of ASR cracks is expected to increase in connection with concrete (mortar) aging. ASR cracks are open, well developed, and several mm thick, in old concrete structures intensively damaged by ASR. By contrast, the initial stage of ASR is characterised by ASR cracks a few μm thick and/or by lines differing in colour, intruding aggregates [2]. Differentiation in the chemical composition of alkali-silica gels was observed in connection with concrete aging, drying, and shrinkage (*e.g.*[2, 65, 129]).

## 4.2. ASR products in real concrete and mortar bar specimens

The following signs, observable on the macroscale, are characteristic of the real concrete structures investigated as a part of this thesis: alkali-silica gels, ASR cracks, and concrete moulding and pulverization. Their *in situ* identification, according to their morphology and colour characteristics, was discussed previously in Section 2, and a detailed description is mentioned in Appendix A and F.

On the microscale, besides alkali-silica gels and ASR cracks (see Fig. 10, 11), the third indicator of ASR is represented by aggregate boundaries attacked by the cement paste. The attacked aggregate boundaries are especially used to identify the ASR of low intensity and age, *e.g.* in mortar specimens (see Appendix C and E). Aggregate boundaries attacked by the cement paste are visible using microscopic techniques in situations in which the ASR initializes. They are

characterised by embayment intruding into the aggregates (see Fig. 11), fully or partially filled with cement paste, and occasionally connected with ASR cracks or alkali-silica gels. The position and shape of the embayment eliminates their origin being in the geological environment or during the aggregate crushing.

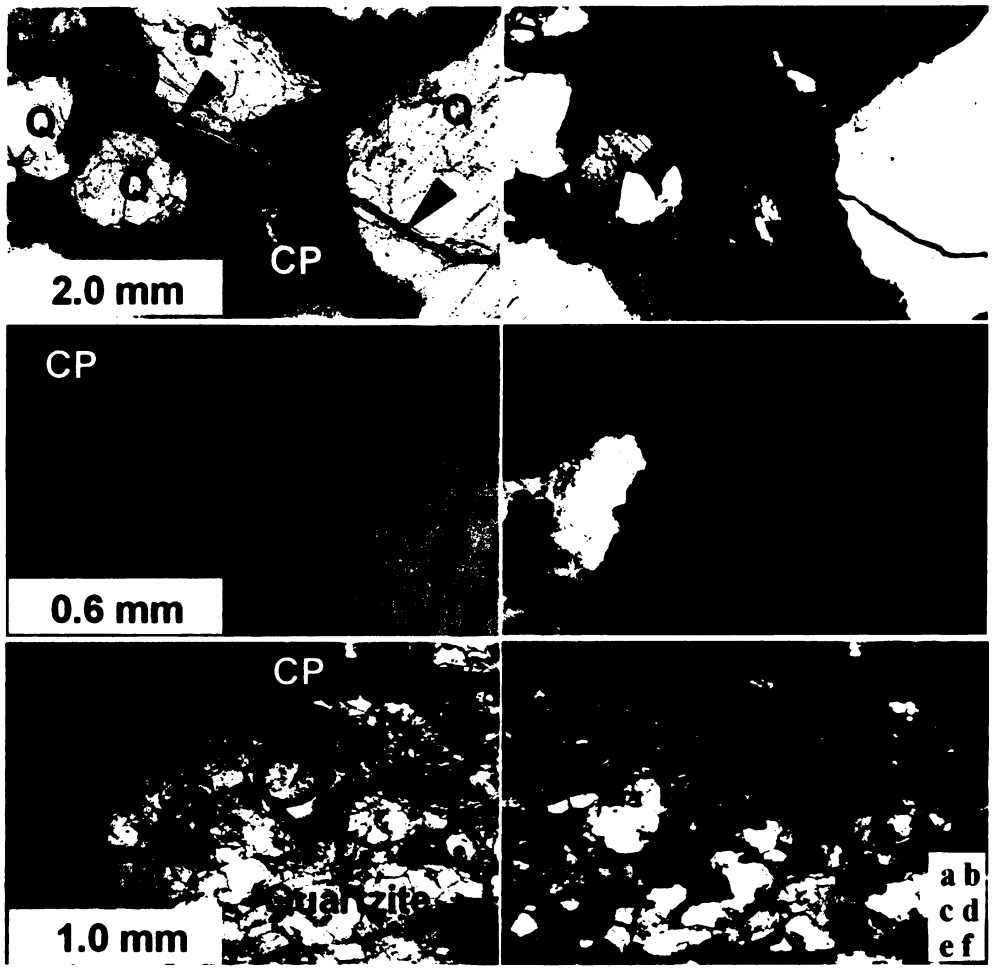


Figure 10. ASR cracks (indicated by blue arrows) and alkali-silica gels (indicated by orange arrows) intruding cement paste (parts a, b), quartz aggregates (parts a, b, c, d), and quartzite fragment (parts e, f). CP – cement paste, Q – quartz. Optical microscope, parallel (parts a, c, e) and crossed (parts b, d, f) nicols. Mortar bar specimen no. 208 (parts a, b, e, f) and gel pat specimen no. 1027T2 (parts s, d). Specimens contain samples of sands and gravels no. 208 (from Roudnice ACHP) and 1027 (from Kaznějov).

In concrete samples containing quartz aggregates with variable mica content and quartzite, specific positions of ASR cracks and ASR attacked boundaries were found (see Fig. 12). Mica (and probably very fine-grained sericite, contained in quartzite and quartz-rich aggregates) is accumulated in sub-parallel layers passing the fragments. These layers are more easily intruded, and represent the positions easily attacked by alkali-silica gels. These conclusions are based on

several observations, but need to be investigated further in the future. A similar conclusion was observed by Broekmans and Jansen [19] in sandstone.

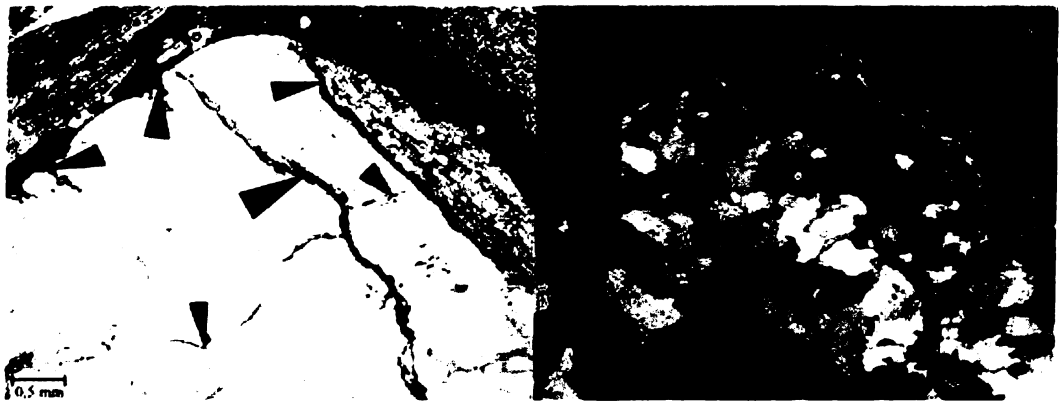


Figure 11. ASR in quartz aggregate exhibited by ASR cracks (in maximum 50 μm thick, indicated by black arrows, connected to mica rich layers), ASR cracks (10-20 μm thick, indicated by orange arrows, without any connection to mica rich layers), and by aggregate boundaries attacked by cement paste (indicated by green arrows). Optical microscope, parallel (on the left) and crossed (on the right) nicols. Concrete sample no. 610-035 from Svijany (constructed in 1924).

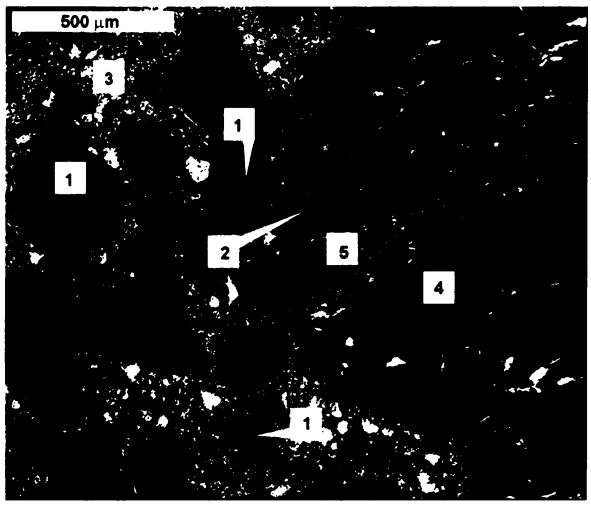


Figure 12. ASR crack (2) intruding quartzite fragment (4) in mica-rich layer (5). The ASR cracks continue into cement paste (3). 1 - alkali-silica gel. SEM/EDS, image in BSE. Concrete sample no. 180-010 from Dolany (constructed in 1934).

The alkali-silica gels are situated partially filling the ASR cracks (intruding aggregates and cement paste) both in pores and in the cement paste. The crystallization of alkali-silica gel is phenomenon dependent on their aging. Crystallized alkali-silica gel show a different structure (the internal structure is more distinctive with clear boundaries), colour (from transparent

tending toward white, to cloudy toward brown and black), and spatial distribution (deposited on aggregate, crack, and pore boundaries). Extensive discussions have been written about the effect of alkali-silica gel aging on its chemical composition [14, 45, 65, 107, 130, 131].

The phenomenon of alkali-silica gels' aging was observed in concrete samples from the 1st half of 20th century, especially in concrete sample no. 180-010 from Dolany, 232-007 from Liblín, and sample no. 610-019 from Tuřice (constructed between 1924 and 1934). The alkali-silica gels exhibit "crystallized" structures (see Fig. 5 in Appendix F) and increasing the CaO / $Na_2O$-$K_2O$ ratio.

A detailed comparison of the alkali-silica gels identified in both the concrete samples and mortar specimens is described in Appendix F. The alkali-silica gels are compared with respect to their chemical composition and morphology. The important differences noted are in regard to:

- Increasing CaO / $Na_2O$-$K_2O$ ratio in alkali-silica gels in concrete samples, in contrast with those from mortar specimens (Fig. 12 in Appendix F).
- Increasing $K_2O$ / CaO-$Na_2O$ ratio in alkali-silica gels in the gel pat specimens, caused by the composition of accelerating solution used during the testing procedure, and composed of NaOH-KOH mixture (Fig. 12 in Appendix F).
- Different structure of alkali-silica gels in older concrete samples (dated to the 1st half of 20th century), in contrast with the usually amorphous structure of alkali-silica gels, identified in younger concrete samples and mortar specimens (Fig. 5 and 6 in Appendix F).
- Increasing CaO / $Na_2O$-$K_2O$ ratio in alkali-silica gels in concrete samples (dated to the 1st half of 20th century), in contrast with those from younger concrete samples.

Our experience from the concrete samples and mortar specimens is in accordance with the data published by Knudsen and Thaulow [14], who correlated the proportion of CaO to the sum of $Na_2O$ and $K_2O$ in the alkali-silica gel, with the age of the concrete, and partially with the position of alkali-silica gel in respect to the surrounding phases. The chemical variability of the alkali-silica gels was investigated in concrete samples by Brouxel [131], who defined the transition zone (rim) formed between alkali-silica gel and the cement paste as 200-250 μm thick. The specific position of the alkalis was found accumulating in the central part of the rim, and rapidly decreasing towards the aggregate.

The low amounts of $Ca^{2+}$ ions in alkali-silica gels from mortar specimens confirms the fact that ASR origin is not only affected by accelerating alkaline solutions (mainly composed of NaOH

and KOH), but also by the $Ca^{2+}$ ions released from cement paste [107]. The effect of $Ca^{2+}$ ions on ASR, and their proportion to other alkalis, was confirmed by Dent Glasser and Kataoka [130] and also by Duchesne and Bérubé [132]. The difficult application of chemical methods in aggregate testing (*e.g.* [22, 52]), which are based on testing in NaOH (or NaOH - KOH) solutions can be partially explained by the effect of $Ca^{2+}$ on ASR.

## 4.3. ASR reaction products – summary

Three main phenomena were observed in respect with alkali-silica gels in real concrete and mortar specimens:

I. Changes in chemical composition of alkali-silica gels, reflecting the composition of their surrounding environment;

II. Influence of aging on the chemical composition of alkali-silica gels;

III. Influence of aging on the morphology of alkali-silica gels.

The observations made as a part of this thesis are in accordance with information published in the literature. The ASR is affected not only by the type of reacting aggregates but also by environmental conditions, the time factor, and the chemical composition of both the cement paste and accelerating solutions. The influence of temperature, atmospheric conditions (the intensity of precipitation), and concrete road de-icing can be expected.

# 5. Summary

**I. Contributions to the methodology of ASR investigations:**

The main contribution of this study is regarded to be the identification of alkali-reactive aggregates, spatially connected with ASR products, by employing petrographic techniques in real concrete (as well as in experimental mortar specimens). Optical microscopy enabled petrographic classification of the aggregates, investigation of their structural characteristics, determination of the volumes of the cement paste and pore voids, and identification of the ASR products. Comparing the methodologies, petrographic image analysis is the only technique allowing quantification of the data obtained during optical microscopy. Conventional optical microscopy is, however, necessary for identification of the phases present. The SEM/EDS method enhances detailed identification of both the chemical composition and morphology of the ASR products.

Based on the concrete investigation, three main groups of methods are significant in the identification of ASR: the *in situ* inspection, defining the extent of ASR on the surface of the concrete constructions; the laboratory macroscopic identification of ASR in concrete samples; and the microscopic investigation. The first two steps affect the selection of sampling points and the selection of the parts of concrete samples to be investigated using microscopic methods.

The identification of ASR in mortar bar specimens is restricted to laboratory methods. The main purpose of the investigation is based on microscopic methods, especially the SEM/EDS method, due principally to the smaller grain size of aggregates and lower extent of ASR in mortar specimens.

**II. Comparative study of ASR signs in different structures**

Alkali-silica gels, ASR cracks, and aggregate boundaries showing an interaction with the cement paste are the most important indicators of ASR. The intensity of individual signs is variable, dependent on both the type of sample and type of reactive aggregates. Based on the relationship of ASR signs to the type of the samples, they can be divided into the two following subgroups:

- Intensive ASR cracks, well visible on the macroscale and frequently intruding aggregates are characteristic of concrete samples. Alkali-silica gels are present in lower volumes, characterised by decreasing $Na_2O/CaO$ content and being partially crystallized.
- ASR cracks are less intensive in mortar bar specimens, rarely intruding aggregates. Alkali-silica gels are contained in higher volumes, characterised by a larger $Na_2O/CaO$ ratio, and strongly affected by the surrounding conditions.

Other divisions of the ASR signs could be seen, based on the type of alkali reactive aggregates:

- ASR caused by the most reactive aggregates, chert-rich limestones, is exhibited by an intensive network of ASR cracks, clearly visible on concrete surfaces. ASR cracks, intruding aggregates and cement paste, are frequently filled by alkali-silica gels. Occasionally, alkali-silica gels are present in "split" form.
- ASR of medium degree is characteristic of slowly reactive aggregates, such as quartz aggregates, quartzite, and quart-rich metamorphic and metasedimentary rocks, identified in older concrete structures. All ASR signs (such as ASR cracks, alkali-silica gels, and aggregate boundaries attacked by cement paste) are well developed, but to a lesser extent than in the previous group.
- ASR of low degree is mainly associated with slowly reactive aggregates, identified in younger concrete structures. According to the position and extension of ASR cracks, and low alkali-silica gels content, it can be deduced as the initial ASR stage. Aggregates are frequently attacked by the cement paste, but ASR cracks have barely developed.
- The last subgroup of ASR signs is characteristic for low or non-reactive aggregates, such as granitoids, serpentinite, or basaltic rocks. ASR cracks are absent. The volume of alkali-silica gels does not exceed 0.1 vol. % and the aggregates are rarely attacked by the cement paste.

The ASR of medium degree is mainly characteristic of concrete samples taken from bridge constructions. In mortar bar specimens, aggregate variability was restricted, due to the testing of quartz sands and gravels, plus the time factor is difficult to simulate.

Our current experience with the signs of ASR points-out the application of quantitative petrographic methods on different rock types, both in real concrete and mortar specimens for future research. In the case of quantitative analysis of the macroscopic ASR signs in concrete constructions, a new methodology is required to be developed. Quantitative determination of

ASR cracks on concrete surface (*e.g.* using the image analysis method) could be a possible solution.

**III. Pilot study of ASR of quartz-rich aggregates in the Czech Republic**

Quartz-rich aggregates of different origins were identified in significant amounts in concrete structures, as well as in experimentally tested quartz sands and gravels. The volume of quartz fragments and aggregates in the investigated samples showed poor or no correlation with the results from the different experimental methods. Detailed petrographic observations of the structural parameters of quartz aggregates, as well as petrographic inspections of these aggregates in concrete samples, showed the following important aspects:

- Very small new quartz grains, originating during a low degree recrystallization mechanism, exhibit important ASR. These aggregates are known as poorly recrystallized aggregates.
- In contrast, well recrystallized coarse aggregates exhibit low or no ASR.
- The ASR potential of quartz-rich aggregates is probably not only dependent on the degree of quartz deformation, but also on the grain size parameters. Both of these factors can be related.

This approach to the reactivity of quartz-rich aggregates seems to be very suitable for future research. Repeated comparisons of recrystallization characteristics of aggregates with their ASR potential can also increase the statistic rigor of the methodology.

**IV. Practical application**

Intensive use of aggregates in the concrete industry points to the importance of their testing. In the Czech Republic, there is a lack of suitable tests and/or the need for validating tests to be revised. The Czech Technical Regulation TP 137, regulating the aggregates testing to ASR, is amenable to new updates. The main conclusions of this study have been summarised and incorporated into Amendments no. 4 and 5 of this regulation.

# 6. References


[1] Hobbs D.W. (1988): Alkali-silica reaction in concrete. London, Thomas Telford.

[2] St John D.A., Poole A.B., Sims I. (1998) Concrete petrography. A handbook of investigative techniques, Arnold, London.

[3] Chatterji S., Thaulow N., Jensen A.D. (1989): Studies of alkali-silica reaction. Part 5. Verification of a newly proposed reaction mechanisms. Cement and Concrete Research 19, 177-183.

[4] Clark B.A., Schwoeble A.J., Lee R.J., Skalny J. (1992): Detection of ASR in opened fractures of damaged concrete. Cement and Concrete Research 22, 1170-1178.

[5] Pearson J.C., Laughlin G.F. (1923): An investigation case of dangerous aggregate. Proceedings of the American Concrete Institute 19, 142-154.

[6] Stanton T.E. (1940): Expansion of concrete through reaction between cement and aggregate. Proceedings of the American Society for Civil Engineering 66, 1781-1811.

[7] Diamond S. (1975): A review of alkali-silica reaction and expansion mechanisms. 1. Alkalis in cements and in concrete pore solutions. Cement and Concrete Research 5, 329-346.

[8] Duncan M.A.G., Gillott J.E., Swenson E.G. (1973): Alkali-aggregate reaction in Nova Scotia: II. Field and petrographic studies. Cement and Concrete Research 3(2), 119-128.

[9] Gogte B.S. (1973): An evaluation of some common Indian rocks with special reference to alkali-aggregate reactions. Engineering Geology 7, 135-153.

[10] Ming-shu T., Su-fen H., Shi-hua Z. (1983): A rapid method for identification of alkali reactivity of aggregate. Cement and Concrete Research 13, 417-422.

[11] Bhatty M.S.Y. (1985): Mechanism of pozzolanic reactions and control of alkali aggregate expansion. Cement, Concrete & Aggregates 7, 69-77.

[12] McConnell D., Mielenz R.C., Holland W.Y., Greene K.T. (1974): Cement–aggregate reactions in concrete. American Construction Institute Journal Proceedings 44(2), 93-128.

[13] Gillott J.E. (1975): Alkali-aggregate reactions in concrete. Engineering Geology 9, 303-326.

[14] Knudsen T., Thaulow N. (1975): Quantitative microanalyses of alkali-silica gel in concrete. Cement and Concrete Research 5, 443-454.

[15] Diamond S. (1993): Alkali-aggregate reactions in concrete: an annotated bibliography 1939-1991. Strategic Highway Research Program, Document SHRP-C/UWP-92-601, Washington.

[16] Bažant Z.P., Steffens A. (2000): Mathematical model for kinetics of alkali-silica reaction in concrete. Cement and Concrete Research 30, 419-428.

[17] Garcia-Diaz E., Riche J., Bulteel D., Vernet C. (2006): Mechanism of damage for the alkali-silica reaction. Cement and Concrete Research 36, 395-400.

[18] Broekmans M.A.T.M. (2004): Structural properties of quartz and their potential role for ASR. Materials Characterization 53(2 - 4), 129-140.

[19] Broekmans M.A.T.M., Jansen J.B.H. (1998): Silica dissolution in impure sandstone: application to concrete. Journal of Geochemical Exploration 62, 311-318.

[20] Zhang X., Blackwell B.Q., Groves G.W. (1999): The microstructures of reactive aggregates, British Ceramic Transactions and Journal 89, 89-92.

[21] Bérubé M.A. (1993): Canadian experience with testing for alkali-aggregate reactivity in concrete. Cement & Concrete Composites 15, 27-47.

[22] Chatterji S. (2005): Chemistry of alkali-silica reaction and testing of aggregates. Cement & Concrete Composites 27, 788-795.

[23] Kerrick D.M., Hooton R.D. (1992): ASR of concrete aggregate quarried from a fault zone: results and petrographic interpretation of accelerated mortar bar tests. Cement and Concrete Research 22, 949-960.

[24] Lu D., Mei L., Xu Z., Tang M., Mo X., Fournier B. (2006): Alteration of alkali reactive aggregates autoclaved in different alkali solutions and application to alkali-aggregate reaction in concrete (II) expansion and microstructure of concrete microbar. Cement and Concrete Research 36, 1191–1200.

[25] Shayan A., Morris H. (2001): A comparison of RTA T363 and ASTM C1260 accelerated mortar bar test methods for detecting reactive aggregates. Cement and Concrete Research 31 (4), 655-663.

[26] Thomson M.L., Grattan-Bellew P.E. (1993): Anatomy of a porphyroblastic schist: Alkali-silica reactivity. Engineering Geology 35, 81-91.

[27] Wigum B.J. (1995): Examination of microstructural features of Norwegian cataclastic rocks and their use for predicting alkali-reactivity in concrete. Engineering Geology 40, 195-214.

[28] Carse A. (1993): The identification of ASR in the concrete cooling tower infrastructure of the Tarong Power Station. Construction and Building Materials 7(2), 117-119.

[29] Fernandes I., Noronha F., Teles M. (2004): Microscopic analysis of alkali-aggregate reaction products in a 50-year-old concrete. Materials Characterisation 53, 295-306.

[30] Jensen V. (2004): Alkali-silica reaction damage to Elgeseter Bridge, Trondheim, Norway: a review of construction, research and repair up to 2003. Materials Characterisation 53, 155-170.

[31] Marfill S.A., Maiza P.J. (2001): Deteriorated pavements due to the alkali-silica reaction. A petrographic study of three cases in Argentina, Cement and Concrete Research 31, 1017-1021.

[32] Bektas F., Turanli L., Ostertag C.P. (2006): New approach in mitigating damage caused by alkali-silica reaction. Journal of Material Science 41, 5760-5763.

[33] Feng X., Thomas M.D.A., Bremner T.W., Balcom B.J., Folliard K.J. (2005): Studies on lithium salts to mitigate ASR-induced expansion in new concrete: a critical review. Cement and Concrete Research 35, 1789-1796.

[34] Kurtis K.E., Monteiro P.J.M. (2003): Chemical additives to control expansion of alkali-silica reaction gel: proposed mechanisms of control. Journal of Materials Science 38, 2027-2036.

[35] Xu G.J.Z., Watt D.F., Hudec P.P. (1995): Effectiveness of mineral admixtures in reducing ASR expansion. Cement and Concrete Research 25(6), 1225-1236.

[36] French W.J. (1991): Concrete Petrography – A Review, Quaterly Journal of Engineering Geology 24(1), 17-48.

[37] Ramyar K., Inan G. (2007): Sodium sulphate attack on plain and blended cements. Building and Environment 42(3), 1368-1372.

[38] Georgali B., Tsakiridis P.E. (2005): Microstructure of fire-damaged concrete. A case study. Cement & Concrete Composites 27(2), 255-259.

[39] Jacobsen S., Gran H.C., Sellevold E., Bakke J.A. (1995): High strength concrete - freeze/thaw testing and cracking. Cement and Concrete Research 25(8), 1775-1780.

[40] Koskiahde A. (2004): An experimental petrographical classification scheme for the condition assessment of concrete in façade panels and balconies. Materials Characterisation 53(2-4), 327-334.

[41] Batic O.R., Milanesi C.A., Maiza P.J., Marfil S.A. (2000): Secondary ettringite formation in concrete subjected to different curing conditions. Cement and Concrete Research 30(9), 1407-1412.

[42] Fu Y., Beaudoin J.J. (1996): Microcracking as a precursor to delayed ettringite formation in cement systems. Cement and Concrete Research 26(10), 1493-1498.

[43] Batis G., Rakanta E. (2005): Corrosion of steel reinforcement due to atmospheric pollution. Cement & Concrete Composites 27(2), 269-275.

[44] Eden M. (2004): The laboratory investigation of concrete affected by TSA in the UK. Cement & Concrete Composites 25 (8), 847-850.

[45] Fernandes I., Noronha F., Teles M. (2007): Examination of the concrete from an old Portuguese dam: Texture and composition of alkali-silica gel. Materials Characterisation 58(11-12), 1160-1170.

[46] Kurtis K.E., Monteiro P.J.M., Brown J.T., Meyer-Ilse W. (1998): Imaging of ASR Gel by Soft X-Ray Microscopy. Cement and Concrete Research 28(3), 411-421.

[47] Peterson K., Gress D., Van Dam T., Sutter L. (2006): Crystallised alkali-silica gel in concrete from the late 1890s. Cement and Concrete Research 36(8), 1523-1532.

[48] Rivard P., Fournier B., Ballivy G. (2002): The Damage Rating Index method for ASR affected concrete – A critical review of petrographic features of deterioration and evaluation criteria. Cement and Concrete Aggregates 24(2), 81-91.

[49] Sahu S., Thaulow N. (2004): Delayed ettringite formation in Swedish concrete railroads ties. Cement and Concrete Research 34(9), 1675-1681.

[50] Bérubé M.A., Samaoui N., Fournier B., Bissonnette B., Durand B. (2005): Evaluation of the expansion attained to date by concrete affected by alkali-silica reaction. Part III: Application to existing structures. Canadian Journal of Civil Engineering 32(3), 463-479.

[51] Pertold Z., Chvátal M., Pertoldová J., Zachariáš J., Hromádko J. (2002): AAR damages of concrete pavement in highway D11 caused by alkali reaction of aggregates (in Czech). Beton 2, 21-24.

[52] Modrý S., Dohnálek J., Gemrich J., Hörbe M. (2003): Elimination of alkali reaction of aggregates in the concrete motorways. Project n. 803/120/114. Czech Technical University, Prague. Unpublished report (in Czech).

[53] ASTM C1260 (1994). Standard test method for potential alkali reactivity of aggregates (mortar bar method). American Society for Testing & Materials, West Conshohocken, Annual Book of ASTM Standards.

[54] DAfStb-Richtlinie (1997): Vorbeugende Massnahmen gegen schädigende Alkalireaktion im Beton (Alkali – Richtlinie). Deutscher Ausschuss für Stahlbeton Ausgebe, Germany.

[55] RILEM (2003): AAR-1 - Detection of potential alkali-reactivity of aggregates - petrographic method. Materials and Structures 36, 480-496.

[56] ČSN 72 1179 (1967): Determination of alkali reactivity of aggregates. Czech Standardization Institute, Prague (in Czech).

[57] ČSN 72 1178 (1968): Chemical analysis of aggregates. Czech Standardization Institute, Prague (in Czech).

[58] ČSN 72 1153 (1984): Petrographic analysis of natural rocks. Czech Standardization Institute, Prague (in Czech).

[59] ČSN 72 1180 (1968): Determination of distinguishable particles of aggregates. Czech Standardization Institute, Prague, (in Czech).

[60] TP 137 (2005): Previous technical conditions – Ministry of Transport CZ and Road and Motorway Directorate of the Czech Republic. Elimination of alkali reaction of aggregates in concrete. Road and Motorway Directorate of the Czech Republic, Prague, (in Czech).

[61] ČSN 72 1160 (1979): Determination of alkali expansion of carbonate rocks. Czech Standardization Institute, Prague, (in Czech).

[62] Johnson N.C. (1915): The microstructure of concretes, Proceedings of the American Society of Testing Materials 15(II), 171-213.

[63] Brown L.S., Carlson R.W. (1936): Petrographic studies of hydrated cements. Proceedings of the American Society of Testing Materials 36(II), 332-350.

[64] Erlin B. (1965): Methods used in petrographic studies of concrete. Analytical Techniques for Hydraulic Cements and Concrete, ASTM STP 395, 3-17.

[65] Haha M.B., Gallucci E., Guidoum A., Scrivener K.L. (2007): Relation of expansion due to alkali silica reaction to the degree of reaction measured by SEM image analysis. Cement and Concrete Research 37, 1206-1214.

[66] Guthrie G.D., Jr., Carey J.W. (1997): A simple environmentally friendly and chemically specific method for the identification and evaluation of the alkali-silica reaction. Cement and Concrete Research 27(9), 1407-1417.

[67] Natesaiyer K., Hover K. (1985): In situ identification of ASR products in concrete. Cement and Concrete Research 18, 455-463.

[68] Natesaiyer K., Hover K.C. (1989): Further study of an in-situ identification method for alkali-silica reaction products in concrete. Cement and Concrete Research 19, 770-781.

[69] Livingston R.A., Aderhold H.C., Hover K.C., Hobbs S.V., Cheng Y.T. (2000): Auto-radiographic methods for identifying alkali-silica reaction gel. Cement, Concrete & Aggregates 22(1), 33 – 42.

[70] Scrivener K.L. (2004): Backscattered electron imaging of cementitious microstructures: understanding and quantification. Cement, Concrete & Composites 26(8), 935-945.

[71] Ponce J.M., Batic O.R. (2006): Different manifestations of the alkali-silica reaction in concrete according to the reaction kinetics of the reactive aggregate. Cement and Concrete Research 36, 1148-1156.

[72] Deceukelaire L. (1991): The determination of the most common crystalline alkali silica reaction product. Materials and Structures 24(141), 169-171.

[73] Bachiorrini A., Montanaro L. (1988): Alkali-silica reaction (ASR) in carbonate rocks. Cement and Concrete Research 8, 731-738.

[74] Gillott J.E., Rogers C.A. (2003): The behaviour of silicocarbonatite aggregates from the Montreal area. Cement and Concrete Research 33, 471-480.

[75] López-Buendína A.M., Climent V., Verdú P. (2006): Lithological influence of aggregate in the alkali-carbonate reaction. Cement and Concrete Research 36, 1490-1500.

[76] Monnin Y., Dégrugilliers P., Bulteel D., Garcia-Diaz E. (2006): Petrography study of two siliceous limestones submitted to alkali-silica reaction. Cement and Concrete Research 36, 1460-1466.

[77] Milanesi C.A., Batic O.R. (1994): Alkali reactivity of dolomitic rocks from Argentina. Cement and Concrete Research 24(6), 1073-1084.

[78] Bork J.B., Christensen P. (1989): Petrographic examination of hardened concrete. Bulletin of the International Association of Engineering Geology 39, 99-103.

[79] Pertold Z., Přikryl R., Lukschová Š. (2007): Identification of ASR in concrete. Faculty of Science, Charles University in Prague. Technical Report (in Czech), p. 70.

[80] Pertold Z., Lukschová Š. (2007, a): Identification of ASR in three concrete samples from crash barrier in Ruzyně. Faculty of Science, Charles University in Prague. Technical Report (in Czech), p. 24.

[81] Pertold Z., Lukschová Š. (2007, b). Quantitative petrographic examination of six concrete samples, colouring methods and identification of ASR in concrete. Faculty of Science, Charles University in Prague. Technical Report (in Czech), p.18.

[82] Pertold Z., Přikryl R., Lukschová Š. (2008): Identification of ASR in concrete. Faculty of Science, Charles University in Prague. Technical Report (in Czech), p. 68.

[83] Horský J. (2007): Concrete degradation in crash barrier „Estakáda Ruzyně". Horský Ltd., Prague. Unpublished report (in Czech), p. 4.

[84] Siegesmund S., Helming K., Kruse R. (1994): Complete texture analysis of a deformed amphibole - comparison between neutron diffraction and U-stage data. Journal of Structural Geology 16(1), 131-142.

[85] Přikryl R. (2001): Some microstructural aspects of strength variation in rocks. International Journal of Rock Mechanics Mining Sciences & Geomechanical Abstracts 38(5), 671-682.

[86] Přikryl R. (2006): Assessment of rock geomechanical quality by quantitative rock fabric coefficients: Limitations and possible source of misinterpretations. Engineering Geology 87(3-4), 149-162.

[87] Martinez-Martinez J., Benavente D., del Cura M.A.G. (2007): Petrographic quantification of brecciated rocks by image analysis. Application to the interpretation of elastic wave velocities. Engineering Geology 90(1-2), 41-54.

[88] Rogers C.A. (1993): Alkali-aggregate reactivity in Canada. Cement & Concrete Composites 15, 13-19.

[89] Wakizaka Y. (2000): Alkali-silica reactivity of Japanese rocks. Engineering geology 56, 211-221.

[90] Shayan A. (1993): Alkali reactivity of deformed granitic rocks: a case study. Cement and Concrete Research 23, 1229-1236.

[91] Bektas F., Turanli L., Topal T., Goncuoglu M.C. (2004): Alkali reactivity of mortar containing chert and incorporating moderate-calcium fly ash. Cement and Concrete Research 34, 2209-2214.

[92] Diamond S., Thaulow N. (1974): A study of expansion due to alkali-silica reaction as conditioned by the grain size of the reactive aggregate. Cement and Concrete Research 4, 591-607.

[93] Hobbs D.W., Gutteridge W.A. (1979): Particle size of aggregate and its influence upon the expansion caused by the alkali-silica reaction. Magazine of Concrete Research 31(109), 235-242.

[94] Mather B. (1975): Durability of concrete construction - 50 years of progress. Journal of the Construction Division - ASCE 101(NCO1), 5-14.

[95] ASTM C295-85 (1985): Standard practice for petrographic examination of aggregates for concrete. American Society for Testing & Materials, West Conshohocken, Annual Book of ASTM Standards.

[96] ASTM C289 (1987): Standard test method for potential reactivity of aggregates (chemical method) - C289-87. American Society for Testing & Materials, West Conshohocken, Annual Book of ASTM Standards.

[97] Grattan-Bellew P.E. (1997): A critical review of ultra-accelerated tests for alkali-silica reactivity. Cement and Concrete Composites 19, 403-414.

[98] Monteiro P.J.M., Shomglin K., Wenk H.R., Hasparyk N.P. (2001): Effect of aggregate deformation on alkali-silica reaction. ACI Materials Journal 98(2), 179-183.

[99] Carles-Gibergues A., Cyr M. (2002): Interpretation of expansion curves of concrete subjected to accelerated alkali-aggregate reaction (AAR) tests. Cement and Concrete Research, 32, 691-700.

[100] CAN/CSA A23.I-M90 (1990): Concrete materials and methods of concrete construction, and methods of test for concrete. Canadian Standards Association, Rexdale, Ontario.

[101] Bérubé M.A., Fournier B. (1993): Canadian experience with testing for alkali-aggregate reactivity in concrete. Cement & Concrete Composites 15, 27-47.

[102] ASTM C227 (1987): Standard test method for potential reactivity of cement-aggregate combinations (mortar bar method) - C227. American Society for Testing & Materials. West Conshohocken, Annual Book of ASTM Standards.

[103] ASTM C 9 -- Proposal -- P 214 (1991): Proposed test method for accelerated detection of potentially deleterious expansion of mortar bars due to alkali-silica reaction. American Society for Testing and Materials, Philadelphia, PA, USA, Annual Book of ASTM Standards, 755-758.

[104] P 18-588 (1991): Aggregates - Dimensional stability test in alkali medium - Accelerated mortar Microbar test. Association Francaise de Normalisation, Paris.

[105] RILEM TC 191-ARP (2003): RILEM Recommended Test Method AAR-0 'Detection of potential alkali-reactivity in concrete' Outline guide to the use of RILEM methods in assessments of alkali-reactivity potential. Materials and Structures 36(261), 472-479.

[106] "PARTNER" (2007): Project "European Standard Tests to Prevent Alkali Reactions in Aggegates", EU-project, http://www.partner.eu.com/index.htm.

[107] Davies G., Oberholster R.E. (1987): Use of the NBRI accelerated test to evaluate the effectiveness of mineral admixtures in preventing the alkali-silica reaction. Cement and Concrete Research 17, 97-107.

[108] Carles-Gibergues A., Cyr M., Moisson M., Ringot E. (2007): A simple way to mitigate alkali-silica reaction. Materials and Structures DOI 10.1617/s11527-006-9220-y.

[109] Qian G., Deng M., Lan X., Xu Y., Tang M. (2002): Alkali carbonate reaction expansion of dolomitic limestone aggregates with porphyrotopic texture. Engineering Geology 63, 17-29.

[110] Nixon P., Sims I. (1996): Testing aggregates for alkali-reactivity, Report of RILEM TC 106. Materials and Structures 29(190), 323-334.

[111] Fournier B. (1993): Recent application of a modified gel pat test to determine the potential alkali-silica reactivity of carbonate aggregates. Cement & Concrete Composites 15, 47-73.

[112] Dudek A., Fediuk F., Palivcová M. (1962): Petrographic tables (in Czech). Nakladatelství československé akademie věd, Prague, 303.

[113] Blatt H. (2006): Petrology: Igneous, Sedimentary, and Metamorphic. W.H. Freeman Edition, New York.

[114] Dolar-Mantuani L. (1983): Handbook of concrete aggregates - a petrographic and technological evaluation. Noyes Publications, New York.

[115] Rayment P.L. (1992): The relationship between flint microstructure and alkali–silica reactivity. In: Poole AB, editor. Proceedings of the 9th International Conference on Alkali-Aggregate Reaction in Concrete, London, UK, (2), 843– 50.

[116] Grattan-Bellew P.E. (1986): Concrete Alkali–Aggregate Reactions. Proceedings of the 7th International Conference on AAR. Noyes Publications, Park Ridge, New Jersey.

[117] Grattan-Bellew P. E. (1992): Microcrystalline quartz, undulatory extinction & the alkali-silica reaction. Proceedings 9th International Conference. The Concrete Society, Slough, 383-394.

[118] del Amo D.G., Perez B.C. (2001): Diagnosis of the alkali-silica reactivity potential by means of digital image analysis of aggregate thin sections. Cement and Concrete Research 31, 1449-1454.

[119] Kwan A.K.H., Mora F.C., Chan H.C. (1999): Particle shape analysis of coarse aggregate using digital image processing. Cement and Concrete Research 29, 1403-1410.

[120] Rivard P., Bérubé M., Olivier J.P., Ballivy G. (2007): Decrease of pore solution alkalinity in concrete tested for alkali-silica reaction. Materials and Structures 40(9), 909-921.

[121] Stipp M., Stünitz H., Heilbronner R., Schmid S.M. (2002): The eastern Tonale fault zone: a "natural laboratory" for crystal plastic deformation of quartz over a temperature range from 250 to 700 °C. Journal of Structural Geology 24, 1861-1884.

[122] Hobbs B.E. (1968): Recrystallization of a single crystal of quartz. Tectonophysics 6, 353-401.

[123] Hirth G., Tullis J. (1992): Dislocation creep regimes in quartz aggregates. Journal of Structural Geology 14, 145-159.

[124] White S.H. (1977): Geological significance of recovery and recrystallization processes in quartz. Tectonophysics 39, 143-170.

[125] Richardson M. (2005): Minimising the risk of deleterious alkali-silica reaction in Irish concrete practice. Construction and Building Materials 19, 654-660.

[126] Hünger K-J. (2007): The contribution of quartz and the role of aluminium for understanding the AAR with greywacke. Cement and Concrete Research 37, 1193-1205.

[127] Indorn G.M. (1961): Studies of disintegrated concrete, Part. I – Progress report. Danish National Institute of Building Research. N3, p. 47.

[128] Diamond S. (1989): Another look at mechanisms. Proceedings of the 8$^{th}$ International Conference on Alkali Aggregate Reaction, Kyoto, Japan, 83-94.

[129] Cong X-D., Kirkpatrick R.J., Diamond S. (1993): $^{29}$Si MAS NMR spectroscopic investigation of alkali silica reaction product gels. Cement and Concrete Research 23, 811-823.

[130] Dent Glasser L.S., Kataoka N. (1982): The role of calcium in the alkali-aggregate reaction. Cement and Concrete Research 12, 321-331.

[131] Brouxel M. (1993): The alkali-aggregate reaction rim: $Na_2O$, $SiO_2$, $K_2O$ and CaO chemical distribution. Cement and Concrete Research 23, 309-320.

[132] Duchesne J., Bérubé M.A. (2003): Effect of the cement chemistry and the sample size on ASR expansion of concrete exposed to salt. Cement and Concrete Research 33, 629-634.

**Appendix A**

# Petrographic identification of alkali-silica reactive aggregates in concrete from 20th century bridges

**Šárka Lukschová, Richard Přikryl and Zdeněk Pertold**

Institute of Geochemistry, Mineralogy and Mineral Resources, Faculty of Science, Charles University in Prague, Prague, Czech Republic.

**Construction and Building Materials (in print)**